Lunar Farside Technosignature & Transients Telescope (LFT3)

DAVID R. DEBOER [ID],[1,2] CHARLIE K. ASHE [ID],[3] OWEN A. JOHNSON [ID],[3,2] EVAN F. KEANE [ID],[3]
ANDREW C. LESH [ID],[4] ELLA J. MARSHALL [ID],[5] STEVE PRABU [ID],[6] KAIA L. REENOCK [ID],[7] ANŽE SLOSAR [ID],[8]
CHENOA D. TREMBLAY [ID],[9,10] JAKE D. TURNER [ID],[11] KARL F. WARNICK [ID],[12]
ANDREW P. V. SIEMION [ID],[6,9,13] JAMIE DREW,[14] AND S. PETE WORDEN[15]

[1]*Sub-department of Astrophysics, University of Oxford, Oxford, OX1-3RH, UK*
[2]*Radio Astronomy Laboratory, University of California, Berkeley, CA, 94720 USA*
[3]*School of Physics, Trinity College Dublin, College Green, Dublin 2, Ireland*
[4]*Department of Civil and Environmental Engineering, Stanford University, CA, 94305 USA*
[5]*School of Physics and Astronomy, The University of Edinburgh, Edinburgh, EH9 3JZ, UK*
[6]*Sub-department of Astrophysics, University of Oxford, Oxford, UK*
[7]*Haverford College, Dept. of Physics and Astronomy, Haverford, PA 19041 USA*
[8]*Brookhaven National Laboratory, Physics Department, Upton, NY 11973 USA*
[9]*SETI Institute, 339 Bernardo Ave, Suite 200, Mountain View, CA 94043, USA*
[10]*Department of Physics and Astronomy, University of New Mexico, Albuquerque, NM 87131, USA*
[11]*Department of Astronomy and Carl Sagan Institute, Cornell University, Ithaca, New York 14853, USA*
[12]*ECE Dept., Brigham Young University, Provo, UT, USA*
[13]*Berkeley SETI Research Center, University of California, Berkeley, CA, 94720 USA*
[14]*Breakthrough Initiatives, 6 Observatory St, Oxford OX2 6EW, UK*
[15]*Breakthrough Initiatives, 9 Rue du Laboratoire, 1911 Gare Luxembourg, Luxembourg*

ABSTRACT

We uniquely rely on radio telescopes to understand the bulk of baryonic matter in the early Universe and the evolution of the Universe across cosmic time to the epoch of reionization. There are two unavoidable limitations to our exploration of the cosmos with terrestrial-based radio telescopes: (1) the prevalence of interfering radio transmitters from human activity, and (2) the Earth's ionosphere and atmosphere, which are opaque or disruptive to many important radio frequency ranges. Both limitations are overcome by reaching above the atmosphere and beyond Earth, a capability that, to date, has generally been the exclusive purview of expensive, government-funded space-based "Great Observatories".

However, we are now on the cusp of a new era, with cost-effective and opportunity-laden access to space (including the lunar surface) becoming a reality. Such unfettered access will enable disparate groups to send instruments there, bringing about a transition from Earth-based observatories to space-based and cislunar telescopes. Although this shift provides exciting opportunities for new science, it will also introduce sources of radio frequency interference (RFI) to the quietest remaining location to which we have access: the lunar farside. Although Earth- or Sun-orbiting telescopes allow for radio frequency measurements below the ionosphere cut-off, they are still exposed to RFI because Earth remains within their line of sight, even at vast distances it can outshine the brightest cosmic sources. Until the Moon's farside becomes crowded with sources of artificial radio emissions, it offers a unique opportunity to measure radiation from the Universe with virtually no interference. The chance to make these

measurements from the lunar farside before it is significantly affected by RFI is unparalleled in human history, but the window of opportunity is limited, and we have a responsibility to future generations to make these measurements. Even in advance of any astronaut activity on the farside, multiple nations are planning constellations of Moon orbiting satellites for science, positioning, and relaying communications, which will inevitably pollute the farside's currently pristine radio environment.

We present here a proposed telescope covering 1 MHz – 2.7 GHz that will land near the lunar antipode within five years to conduct baseline observations free from RFI. The Lunar Farside Technosignatures and Transients Telescope (LFT3) will search the farside sky for radio emissions from known and unknown sources, and create a historical record of lunar radio observations as the current silence gives way to a more crowded RF environment with the deployment of additional instruments. LFT3 is the *only* mission across this band proposed to take advantage of this unique opportunity in human history.

1. INTRODUCTION

Despite numerous efforts to decipher its origin (for example, Méndez et al. 2024; Perez et al. 2022), the "Wow!" signal (Ehman 2008) remains among the most tantalizing unexplained radio signals today. This signal, seen in 1977 and rendered as "6EQUJ5" on the observatory printout, was unmistakably detected and aligned with the expected sidereal signal through the telescope beam, strongly implying an origin in deep space. At the time, the world had few transmitters in air or space, allowing the signal to stand out. However, in today's world, this signal would be lost in the cacophony of our technological emissions that permeate the sky. Given all of this, the signal remains enigmatic to this day (Saide et al. 2023; Haqq-Misra et al. 2025; Sheikh et al. 2025). Since it was only seen once, conclusive evidence of its origin has not been determined, which could have been anthropogenic or something more. Imagine going to a place where literally everything seen is of scientific interest and being able to explore it using modern technology that is far more advanced than the telescope used in 1977. That is the promise of a lunar farside telescope.

Humanity is at a tipping point for conducting effective radio-astronomical observations from Earth. The ever-increasing use of wireless communication devices on the ground and in orbit means that nowhere on our planet, even remote locations with very low population density, is free of significant radio frequency interference (RFI). Although we have previously launched a small number of expensive "Great Observatories" into space, the increasing affordability and accessibility of space technology now make it feasible to deploy a large number of smaller telescopes. We are therefore at the edge of the transition from earth-based to space-based radio astronomy, born from the need to respond to changes in Earth's radio frequency environment, as well as the increased scope needed for scientific advancement. Making observations above the Earth's atmosphere and ionosphere also opens up observing windows inaccessible from Earth.

However, in this transition to space, we risk injecting the same RFI into these new domains. This is particularly true for the lunar farside, with its unique feature of always pointing away from the Earth providing essentially perfect shielding from the Earth (Maccone 2019; Michaud et al. 2020; Heidmann 2002). This makes it urgent to get well-designed sensors there as soon as possible to make early baseline measurements and conduct the unique science allowed only by its essentially RFI-free environment. The lunar farside represents a unique opportunity in human history for quiet, high-quality observations Bassett et al. (2020), but this window will soon close as the increasing scientific and political interest in lunar exploration brings new assets to the moon, as seen in Figure 1. Figure 2 assumes appropriate orbits and lifetimes for the missions
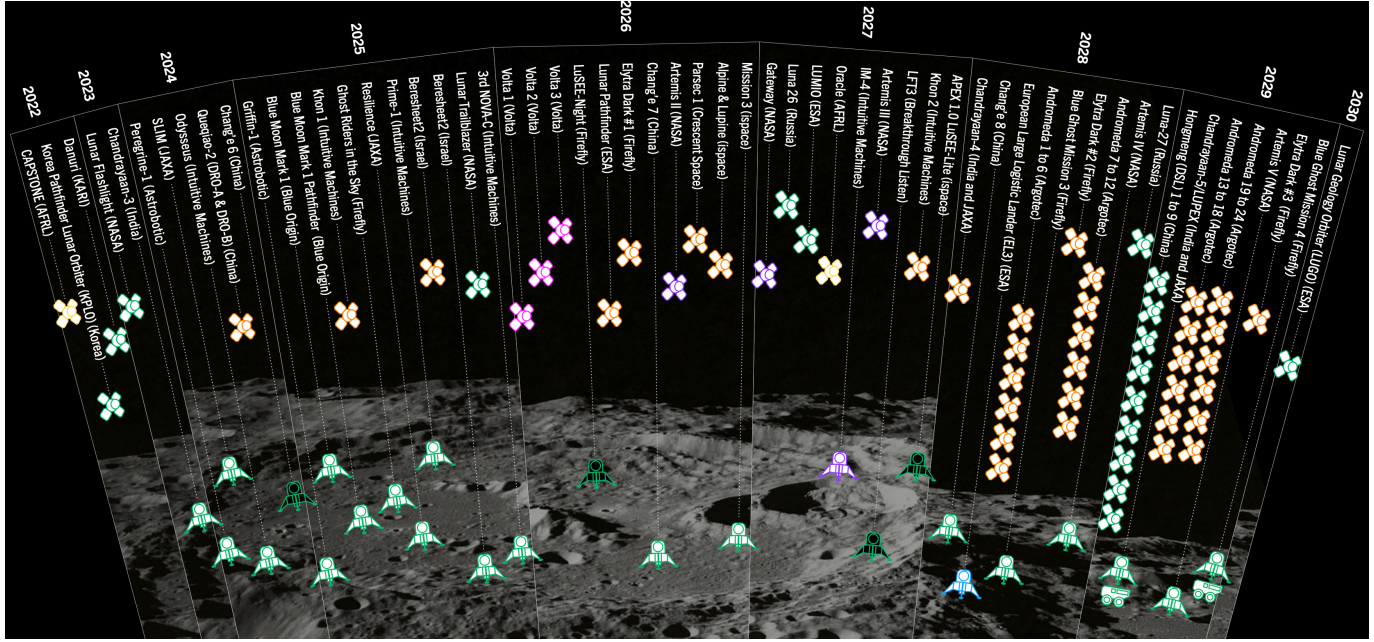
Figure 1: Graphic showing previous and planned cislunar missions with multiple objectives, as listed in the legend.
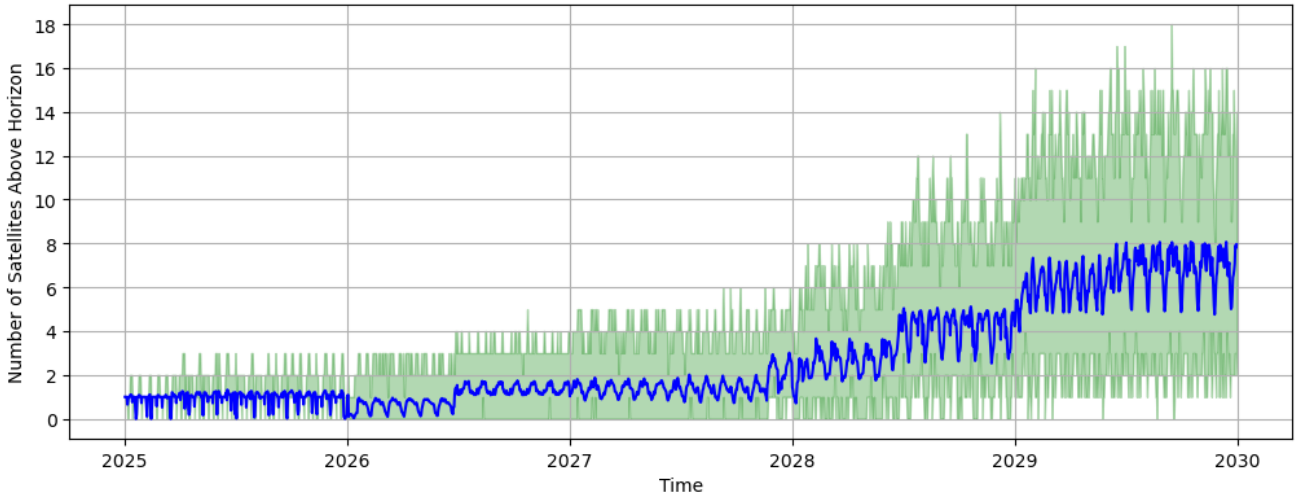
Figure 2: Plot of the number of satellites above the horizon as a function of time. The green area is the minimum and maximum above the horizon at any given time over a day, while the blue line is the average number above the horizon in that day. Note that by mid-2028, there are significant portions of time where there is always a satellite above the horizon.

and shows the number of satellites above the horizon. The green area shows the minimum and maximum number of satellites in a day, while blue is the average over that day. Beginning in mid-2028, there are significant periods of time when there will always be a satellite above the horizon.

To act on this singular opportunity, we propose a radio telescope to be landed near the lunar antipode within five years to conduct these unique-in-history measurements. The telescope will comprise a suite
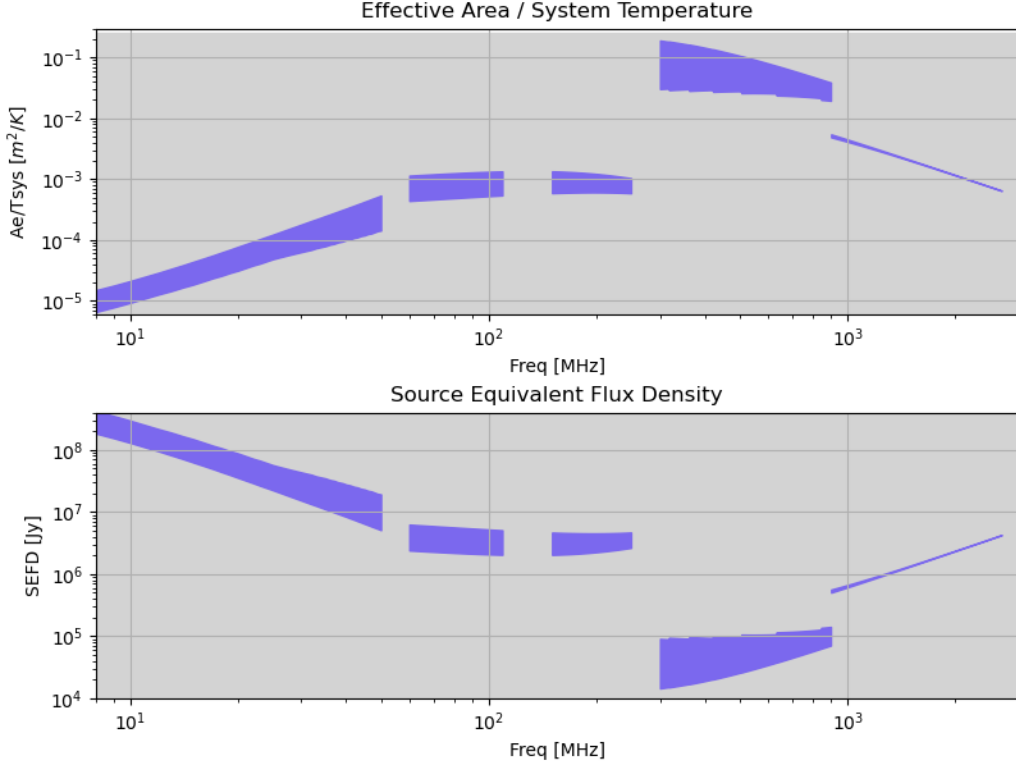
Figure 3: Frequency bands of LFT3 and their associated sensitivity in terms of effective area over system temperature (top) and source equivalent flux density (bottom). The range stems from different fields over the varying sky temperatures due to Galactic emission and the plot is for the day-time powered system.

of antennas and arrays designed to cover a wide range of frequencies and be of a scope that would allow for quick and cost-effective deployment in that timeframe. Deploying and operating from the lunar farside introduces several system constraints. Key limitations include a total payload of approximately 100 kg, power consumption of 100 W during the lunar day, and data transmission of 100 GB/month back to Earth. Therefore, the system design and scientific objectives discussed in this document are subject to these system constraints.

The primary instrument is a UHF dual-pol multibeam phased array operating at $300 - 900$ MHz. This band corresponds to a sensitivity maximum set by the increasing Galactic noise with decreasing frequency and the smaller collecting area for an array of this physical and fiscal scope as you increase frequency. A smaller array operating at $900 - 2700$ MHz will allow a large band to be surveyed and will also allow the measurement of S-band communication signals from the Moon and potentially Mars. Individual antennas will cover HF ($1 - 50$ MHz) and VHF in two bands, $60 - 110$ MHz and $150 - 250$ MHz. Note that at HF and VHF frequencies and for the scope of this mission, multiple antennas per band provide little to no benefit. The mix of these receivers is unique to all other proposed missions and is well served by the stable and always shielded lunar farside location (Burns et al. 2021a).

Figure 3 shows the frequency bands and their expected sensitivity, and Table 3 provides an overview of the system. During its mission lifetime, the telescope will observe most of the sky (see Fig. 4) and conduct historical surveys in the solar system's most RFI-pristine environment before the presence of humanities' technology increases the radio frequency interference, even at this very remote place. By the end of the decade it is likely that several dozen spacecraft will be orbiting the Moon, so time is limited.
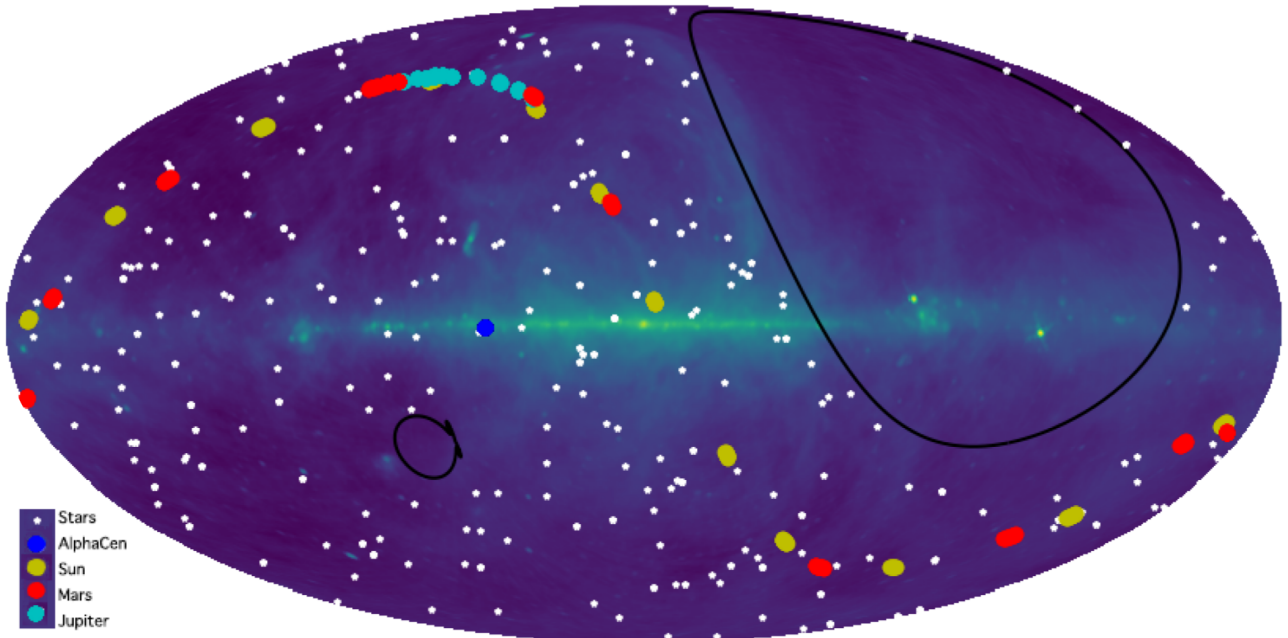
Figure 4: Graphic showing the field-of-view of LFT3 over the calendar year 2028 imposed over a graphic of Milky Way emission at 650 MHz (Price 2016). The white points represent the stars within 10pc and the blue circle is Alpha Centauri. The yellow circles are the Sun's position as seen over the year. The red circles are Mars over that period and the cyan circles are Jupiter. The interior region of the black shapes are outside the field-of-view.

In addition to the RFI considerations at radio frequencies, which can be extensive even in remote Earth locations, as shown in Figure 5, there are other very significant scientific reasons for operating a radio telescope on the farside of the Moon. The ionosphere surrounding our planet creates a conducting medium through which electromagnetic radiation is impeded at frequencies below about 10 MHz and distorted below about 30 MHz[1] (e.g. Zawdie et al. 2017) and for this reason low frequencies remain the last unexplored region of the electromagnetic spectrum. Due to the absence of a tangible ionosphere on the moon, there are no technical barriers to studying physics at these new and unexplored frequencies. The primary motivations for targeting the lunar farside– getting above the atmosphere and away from RFI– are central to the design of the system.

Note that RFI manifests itself in different ways, depending on its strength and an instrument's ability to handle it. There are four basic RFI regimes[2] (e.g. Ellingson 2005, Selina & De Pree 2023):

- *Saturation*: Strong RFI that drives the receiver into saturation and creates problems throughout the band, effectively rendering it unusable. This must be avoided at all costs by instrument design and operational constraints. Avoidance is increasingly difficult to achieve due to increasing RFI sources, such as large satellite constellations.

---

[1] The impacted frequencies vary in time and place and are also a function of solar activity.

[2] A new and emerging approach may be called "cooperative RF", whereby services coordinate their use – this approach is being pursued by the US National Science Foundation in its National Radio Dynamic Zone research.
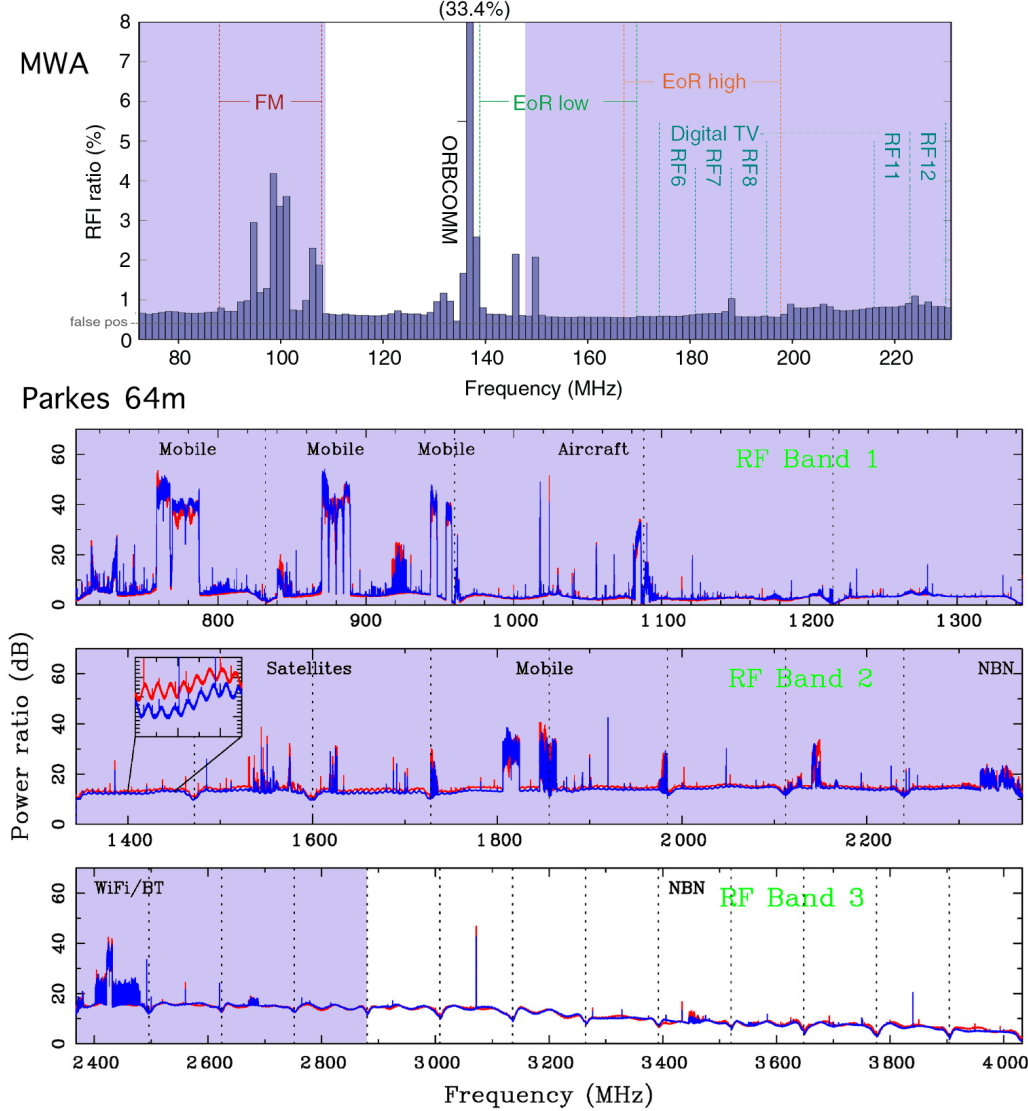
Figure 5: Figure showing the RFI environment at the Murchison Widefield Array (MWA; Offringa et al. 2015) and the Parkes 64m (Hobbs et al. 2020) telescopes. Highlighted are the regions proposed for use by the lunar telescope. This represent examples of the challenges ground-based observatories face when doing observations in the presence of RFI. The MWA site is government protected for radio astronomy, and even in this scenario RFI can still dominate certain regions of the spectrum and limiting the science outcomes.

- *Coherent mitigation*: If the receiver is not overly saturated with strong RFI and if the characteristics of the interferer are known or retrievable, it is possible, in some cases, to mitigate by subtraction or suppression of the interferer. This has largely been in the research rather than operational realm given its difficulty and its effect on the science data. It may be useful in the future for certain science goals, such as detecting transients such as pulsars and fast radio bursts (FRBs), or with widely separated coherent receivers. Another technique is to orient the array's blid spots (nulls) towards known sources of RFI as a mitigation technique.

- *Identification and excision*: As in the case above, if the receiver is not in significant compression and if the RFI can be identified (taking into account harmonics), it may be removed or "flagged",

with a resultant loss of data. This is by far the dominant technique used in radio astronomy. This technique generally allows some science to proceed; however, it provides a scientific limit and a loss of discovery opportunity.

- *Low-level*: This is the insidious presence of low-level RFI that is below the threshold of identification and excision. It provides a low-level noise floor that is essentially unknowable and is a particular issue for extremely high-sensitivity cosmological global experiments. Observing at these frequencies without low-level RFI is a unique aspect of the lunar farside.

Lunar farside observations are currently free from all of these aspects of RFI, representing our only chance of observing without the low-level RFI noise that impacts sensitive radio astronomical measurements in all other environments.

When considering this endeavor, some other factors should be considered:

- At low frequencies, the system temperature will be dominated by Galactic noise and impulsive events will be affected by scattering and dispersion. Any civilization generating a beacon will be aware of this constraint regardless of where they are located in the Galaxy, which tends to discourage arguments for low-frequency SETI. However, this is the last unexplored region of the electromagnetic spectrum and should be thoroughly observed.

- Having the widest possible absolute bandwidth and largest feasible field-of-view will maximize the possibility for serendipitous discoveries, particularly of rare events.

- The possibility of initial discovery of technosignatures in the aforementioned bands with Earth-based telescopes is drowned out by "anthropogenic technosignatures" aka RFI. The lunar farside should be completely devoid of this for at least 5 years.

- LuSEE-Night will operate from the lunar farside at radio frequencies (0.1-50MHz) that are below the Earth's ionospheric cut-off to make radio astronomical observations impossible, which can be augmented by this telescope.

- An all-sky monitor from the lunar surface will give an unprecedented view of bright but rare transient events, including those obscured by the atmosphere and RFI from Earth.

- Our window for collecting interference-free legacy spectra is brief. By 2030, more than a dozen satellites are expected to orbit the Moon, significantly increasing RFI on the lunar farside.

- The unique scientific payload on the lunar farside is always shielded from Earth's RFI and has longer sky dwell times due to the slow lunar rotation.

We note that an observatory on the farside of the moon has no visibility of Earth, and thus would have limited use for military or intelligence purposes, emphasizing its exclusively peaceful, scientific mission. The radio quietness of the lunar Farside was demonstrated in 1975, with the RAE-2 spacecraft (Alexander et al. 1975). This remained the only such demonstration until China conducted measurements with the Longjiang-2 orbiter in 2018 (Yan et al. 2023). It is time to land a telescope to take advantage of this opportunity. Potential science cases for bringing this telescope to life are outlined in the next section, followed by a discussion of the payload and operational model. A discussion of other potential telescope locations and options is then discussed, demonstrating the unique qualities of the lunar farside for this mission.

2. SCIENCE CASE

The lunar farside provides a unique radio frequency (RF) environment in our Solar System in that the moon shields it from Earth and near-Earth RFI at all times. Therefore, *anything* detected there is of scientific interest. Since there is no ionospheric blockage, low-frequency observations that are impossible from Earth can also be made in this RFI-free environment.

Note that the science case contains science from a number of categories: (1) science where LFT3 can do unique science that cannot be done or done as well from Earth; (2) science where LFT3 provides useful information that could be used in addition to observations that can be done from Earth; (3) science that demonstrates that LFT3 works and provides confidence in the performance of the telescope and lunar operations. For guidance, the science case is *not* predicated on what might be done if one had a large budget to design and build a radio telescope on Earth, but rather what could one do for an inexpensive lunar mission that advances science and our understanding of operating on the moon.

Although the lunar farside is currently a low-RFI site, *now* is the only time to take completely pristine measurements of the radio spectrum. This is an opportunity that will never again present itself, as seen in Figures 1 and 2, with more than three dozen lunar orbiters planned before 2030. This section discusses the primary science cases that drive the design of the array, which are summarized in the science traceability matrix in Appendix A.

2.1. *Technosignatures*

Humanity's quest to determine its place in the Universe and whether we are its only inhabitants has driven our imagination and quest for knowledge since we first looked to the sky. Many large telescopes across the electromagnetic spectrum are being planned and developed to help determine if biological processes are happening around nearby stars (called "biosignatures"). We now also have the capability to explore whether technological signals ("technosignatures") exist over a large swath of our Galaxy. The Breakthrough Listen program (Worden 2016) has transformed the field and has greatly expanded the search for such technosignatures (e.g. Enriquez et al. 2017; Price et al. 2020; Gajjar et al. 2021). The greatest technical impediment in this endeavor is the prevalence of RFI made by essentially every device on and around Earth that is electrically powered.

Although RFI is prevalent, excellent technosignature searches can be conducted from the Earth, particularly from remote locations where terrestrial interference is low and at frequencies that, at that time and place, are free of interfering signals. Excision techniques, as mentioned above, are generally used to flag RFI based on statistical methods and can be very effective. However, it is noted that technosignatures, being of artificial origin, have characteristics similar to RFI and may be thrown out in this process, and that excision also represents an opportunity lost to making a detection. The prevalence of RFI also renders any eventual detection less certain as any signal could be the result of pathological RFI. The recent experience of Breakthrough Listen Candidate 1 highlights this (Sheikh et al. 2021).

Figure 6 provides a high-level summary of the coverage of ground-based radio searches, both ongoing and completed (circles). The purple and red-shaded regions show two of the large program ground-based technosignature searches currently in progress. For Earth-based searches, in order to further guard against interference, one usually uses a cadence of a series of on-target and off-target observations, where the "off" can be the "on" for another target. The use of this in a multibeam system like LFT3 is demonstrated in Huang et al. (2023). Using a multibeam system allows "on" and "off" to be simultaneous, making it even more efficient (i.e., Luan et al. 2023). Also, note that a remote site does not provide shielding from satellites
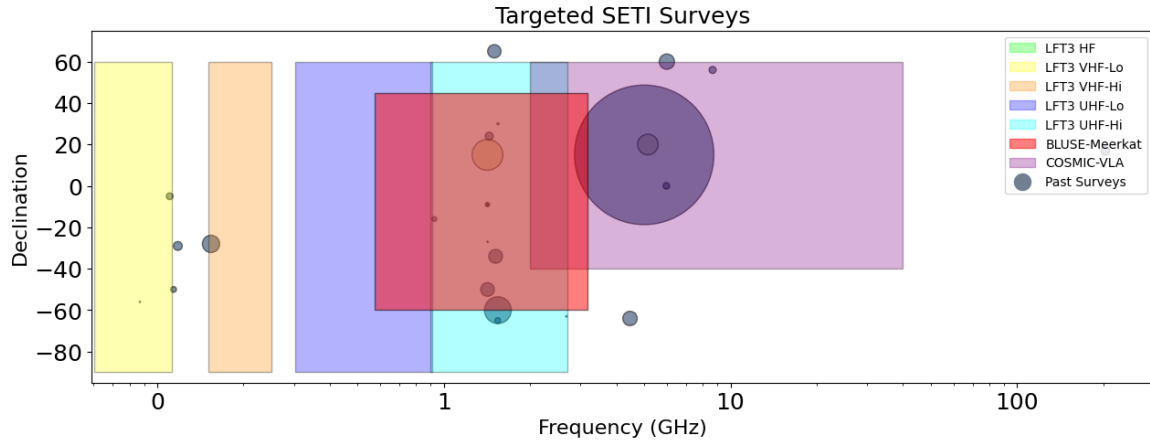
Figure 6: A plot of the historical technosignature searches (modified from Tremblay et al. 2022). The list of surveys are compiled drom https://technosearch.seti.org/radio-list. The circle size is scaled to the total number of targeted sources within the survey and located at the average declination. The colored rectangles show the regions in frequency and declination that LFT3 will cover as well as two large ground-based programs conducted by Breakthrough Listen and SETI Institute. As shown, LFT3 will survey regions that cover both new or rare regions (HF and VHF) as well as well-studied regions (UHF).

and airplanes. Techniques exist to subtract or decorrelate interference, but they are not perfect and it seems unlikely that a technosignature detection "through" RFI would be believed, even if not immediately rejected in a pipeline, as would likely be the case.

Of course, we have no a priori information on any parameter of a technosignature, so one must search agnostically with the most sensitive receivers one can muster. However, we submit that the initial signal detected will likely have a relatively high signal-to-noise ratio in some parameter space. For now, at radio wavelengths, that parameter space generally comprises frequency and time, and narrow-band or pulsed signals are the most likely to be detected. They are also among the least likely signals to be confused with an astrophysical process (Hippke & Forgan 2017), but are most likely to be confused with RFI. Within that parameter space, there is a case to be made that the most likely initial detection will be a slow transient arising from some underlying cadence such as a civilization targeting many distant worlds with a beacon or some fortuitous alignment such as the conjunction of two extrasolar planets with our telescope beam. As mentioned in the Introduction, the "Wow!" signal is an exemplar of what one such signal could look like. As also mentioned, if observed from Earth, even if that event occurred when it was not obscured by RFI, one would likely not have a high confidence of its origin due to the many sources of potential RFI. To reliably detect such a signal, one must go to a place where no other potential sources of emission reside.

In order to assess whether a small telescope can meaningfully search for technosignatures, it is instructive to look at detectability of various transmitter strengths for the stellar distribution around us. The Arecibo planetary radar (when it was operating) had been the highest effective isotropic power radiator at a level of greater than 20 TW and is a key fiducial. Another is to assume that an advanced civilization could produce significantly greater radiated power; in this case we will consider 1000 times that of the Arecibo planetary radar (Gray 2020). Figure 7 shows LFT3's sensitivity towards nearby star systems. As shown, even *our* current technology (such as the Arecibo Planetary Radar System) provides a detectable signal to this telescope, let alone a stronger signal from a more advanced civilization.
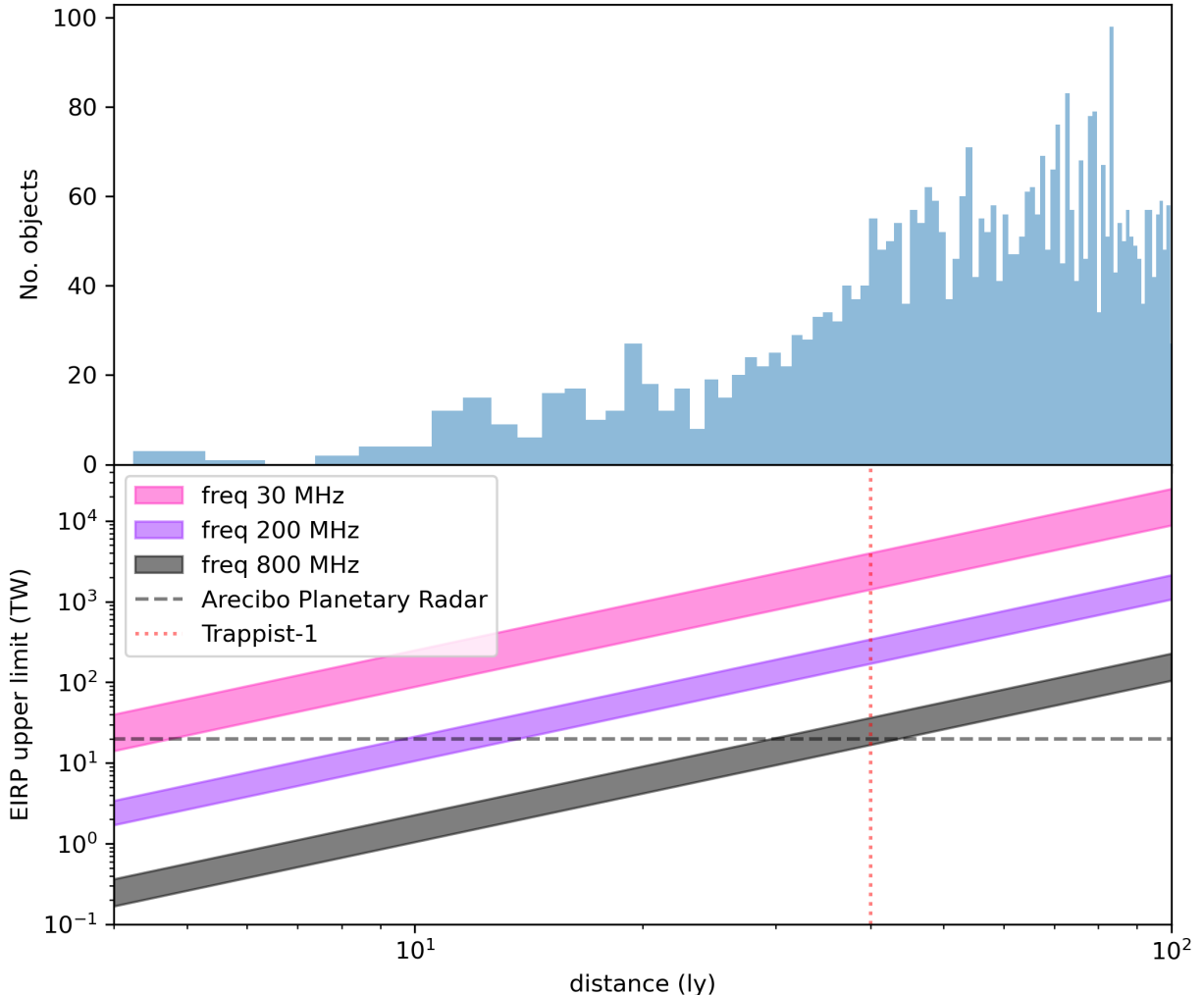
Figure 7: In the top panel we show list of objects within 100 light years complied together for technosignature studies with LFT3. We direct the reader to (Prabu et al. 2025b) for more information on about the combined catalog of stars for LFT3. Bottom panel shows the ERIPs probed by LFT3 at different frequencies as a function of distance. We note that that the Arecibo Planetary Radary System placed at the Trappist-1 system would be detectable by LFT3.

System Implications: As shown in Figure 6, the proposed telescope frequency range covers a new parameter space in technosignature searches, especially with HF and VHF receivers. Technosignatures may emit into a single polarization state and therefore polarization sensitivity is needed. The technosignature science case requires some in-line processing of the data to find signals of interest and generation of dynamic spectra or raw voltage postage stamps around signals of interest. In the commensal system, real-time is used in MeerKAT (Czech et al. 2021) and VLA (Tremblay et al. 2024), SETICORE [3] to search for signals toward beam-formed targets. SETICORE uses an efficient Taylor-Tree de-dispersion algorithm to autonomously search for narrowband signals. The user specifies the signal-to-noise ratio to identify signals of significance and the drift-rate search width. To save on information needing to be transferred to the ground, one could

[3] https://github.com/lacker/seticore

de-disperse the signal and only transmit the time averaged power spectrum instead of sending the entire dynamic spectrum. As there is no known technosignature signal thus far identified, frequency resolution and time resolution are open parameters that are flexible to the needs to keep data rates and processing to a minimum. Section 3.2 will outline the concept of operations given the highly constrained mission parameters. The nominal specifications are 1 sec time resolution and 10 Hz frequency resolution. Recently, it has been suggested that narrow spectral lines may be additionally broadened by coronal activity of the local star (Gajjar & Brown 2025), better matching these somewhat larger spectral bins.

We can verify these modes of operation by looking toward Mars, where there are a number of space-based and ground-based communication signals transmitted back to Earth on a regular basis, as well as for lunar orbiters. The carrier signals are typically emitted at 2200-2290 MHz and represent a population of narrow-band artificial signals. The sky rotates $\approx$ 30 times slower when observing from the Moon's surface compared to Earth. This allows longer dwell times on a given patch of sky, which in turn allows prolonged studies of signal characteristics.

2.2. *Transients*

In the last 20 years, the field of radio transients (both slow and fast) has brought a wealth of information, significantly advancing various areas of physics. In particular, pulsars and fast radio bursts (FRBs) stand out because of their unique potential to reveal new types of physics (Beskin et al. 2015; Ng 2023) and understanding of the fabric of spacetime (Lyne et al. 2004). These astrophysical phenomena offer valuable insight into gravitational waves, cosmology, and plasma physics, among other fields. However, radio observations can also shed light on other transients, such as flare stars and planetary conditions within the Solar System. Overall, the strength of a lunar-based telescope is in discovering the unknown. This includes the possible detection of various 'low-DM' (or dispersion measure, an indicator of relative proximity) events, on timescales of milliseconds to minutes. Such events may include low-DM FRB analogues, FRBs from Galactic magnetars, decimetric solar bursts, stellar bursts, and undiscovered time-domain phenomena. In particular, LFT3 would uniquely enable the discovery of new populations of transient astrophysical sources in the very local Universe at 0–30 MHz and 87–108 MHz. Figure 8 details various observational setups of LFT3 against well-known transients in the νW vs L_ν (Where νW represents the product of observed frequency and pulse width and L_ν shows the spectral luminosity) parameter space along with minimum detectable flux density values at various pulse widths. Here it is important to note that this is the average flux density of these objects, in reality these objects adhere to a flux distribution where higher and lower flux values will be emitted.

2.2.1. *Solar Physics*

Low-frequency studies of the Sun date back to the early days of radio astronomy, with some of the first published observations appearing in the 1940's (Payne-Scott et al. 1947; Wild et al. 1963). Despite this early start, a new generation of instruments, including LOFAR and the MWA, has enabled significant advances due to wider bandwidths, improved telescope design, and enhanced computational capabilities. Key science goals include the study of non-thermal emissions, gyrosynchrotron emission associated with coronal mass ejections (CMEs), targeted analyses of solar bursts (Types I–V), and polarimetric measurements (Valio et al. 2013). Many of these studies require high-bandwidth imaging on short time scales (Kansabanik et al. 2022), though the spectral-temporal characteristics of quiescent versus active solar states are also of interest given their impact on Earth-based technologies.
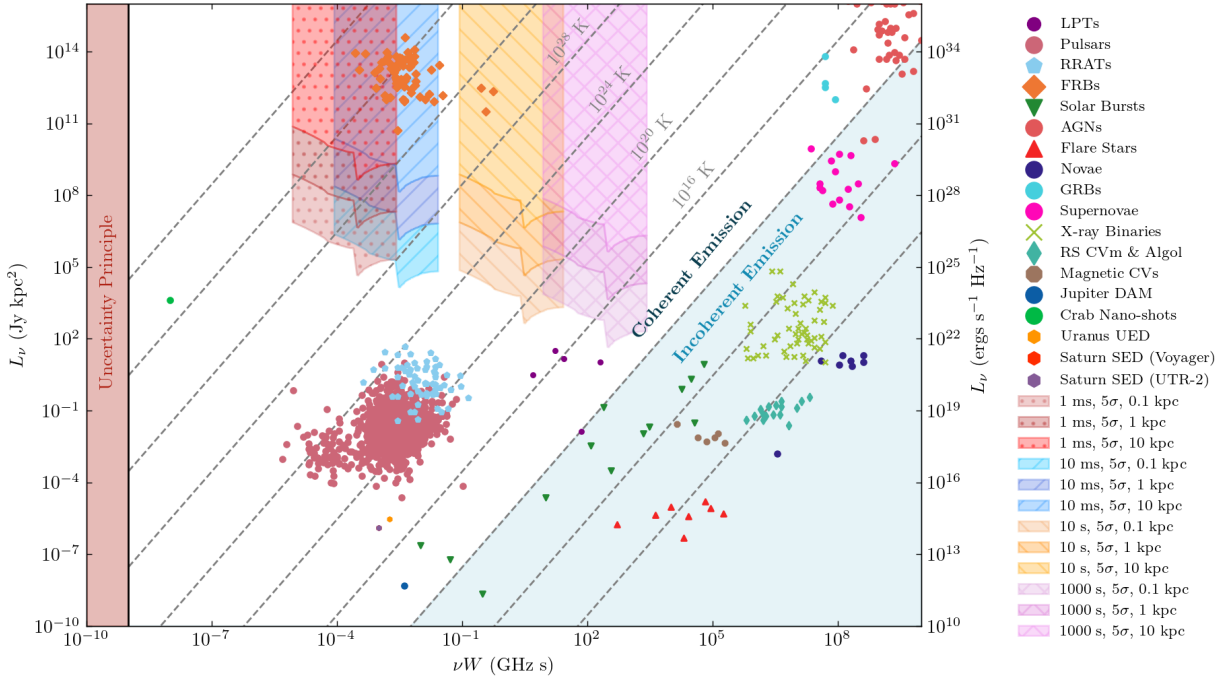
Figure 8: Transient Parameter Space figure adapted from Pietka et al. (2015). This plot illustrates the sensitivity regions of a LFT3 observational setup across different pulse widths (1 ms, 10 ms, 10 s and 100 s) up to 10 kpc on a νW vs. L_ν phase diagram. Where νW represents the product of observed frequency and pulse width and L_ν shows the spectral luminosity. The blue, green and red hashed regions correspond to a pulse width and show the detectable signal levels above a threshold of 5σ for the LFT3 bandwidth.

One of the significant outstanding questions in heliophysics is: "How does the Sun produce strong southward-pointing magnetic fields in solar CMEs that lead to geomagnetic storms, and can such storms be predicted?" In an effort to explore the connection between CMEs and phenomena such as Type II bursts, solar flares, and shocks, Bastian et al. (2001) analyzed observations at 150 and 450 MHz with 32 s integration and ~1 MHz spectral resolution. Their work yielded constraints on thermal plasma density, density filling factors, relativistic electron number density, and magnetic field strength within CMEs – values still widely referenced today.

Solar observations at varying time and frequency resolutions remain challenging. A farside lunar telescope would offer a dynamic spectral view of solar activity across a frequency range unobservable from Earth and not explored in detail since the Voyager missions of the 1970s. As the Sun approaches solar maximum, such a telescope would be uniquely suited for capturing transient low-frequency events, such as Type II/III bursts and solar-driven auroral emissions from planetary bodies.

Interplanetary scintillation (IPS) observations from the lunar farside could be used to pinpoint solar wind and heliophysical structures by measuring the rapid intensity fluctuations of the compact radio background caused by turbulence in density regularities in the solar wind (Fallows et al. 2023). This technique could potentially reveal bulk flow velocities and turbulence levels and detect large-scale heliospheric density structures (e.g., tracking CME-driven shocks) throughout the inner heliosphere. Compared to Earth-based IPS

experiments [4] that are limited by terrestrial ionospheric distortion, LFT3 could lend its low observing frequency phased array to achieve higher angular resolution (Brinkerink et al. 2025).

System Implications: High-time-resolution dynamic spectra with time resolution on the order of 1–2 ms and spectral resolution of ≤ 0.5 MHz would be critical for resolving fast-evolving solar radio bursts, particularly Type III. Coherent bursts from solar events can reach flux densities of $\sim 10^3$–10^6 Jy, but occur over narrow frequency bands and short durations, requiring fine temporal and spectral sampling for full characterization. Dynamic spectra in both Stokes parameters I and V would allow for polarimetric studies of coronal magnetic fields and emission mechanisms. Low-frequency IPS studies require long integration baselines (e.g., 10–100 s) across a wide field of view to track scintillation patterns and infer bulk solar wind properties and density turbulence.

The frequency range of interest spans $\sim$0.1–30 MHz, encompassing the decametric and hectometric bands relevant for Type II/III solar bursts and the IPS regime. This range lies entirely below Earth's ionospheric cutoff, making space deployment essential. A phased array configuration with beam steering would facilitate flexible observation of both targeted and wide-field events. Coordinated observations with MWA, LOFAR, and space-based platforms like SunRISE would enable multi-instrument solar diagnostics across a broader frequency range and heliocentric baselines. These data products would be valuable across both active and quiescent solar phases, contributing to long-term solar monitoring and forecasting of geomagnetic activity.

2.2.2. *Solar System Emission*

There exist numerous sources of radio emission throughout the solar system. Most notably, Jupiter's strong magnetic field interacts with its moons, particularly Io (Goldreich & Lynden-Bell 1969), but also Europa and Ganymede (Zarka 1998; Louis et al. 2023), producing intense MJy-level auroral radio emissions. Jupiter emits over a broad frequency range from 10 kHz to 40 MHz (Zarka 1998), with its hectometer-wavelength (1–5 MHz) emission modulated by solar wind activity (Desch & Barrow 1984). The electron cyclotron maser instability (ECMI; Zhelezniakov & Zlotnik 1975), a plasma instability that occurs in magnetized environments with energetic electron populations, is the main driver of the Jupiter emission (Zarka 1998). Jupiter is the only planet in the solar system[5] whose ECMI radio emission can be seen from the ground due to the ionsphsheric cuttoff (Zarka 1998). A lunar-based telescope would enable observations of these low-frequency bands, particularly around solar maximum, offering an opportunity to study solar-wind-driven dynamics in the Jovian system. This study can also be used as a benchmark for studying exoplanet radio emission from close-in exoplanets (Zarka 2007; Callingham et al. 2024).

A lunar telescope is also well suited to probe low-frequency emission generated by lightning from the solar system. In particular, LFT3 can study the radio emissions generated by lightning from Venus, Mars, Saturn, Uranus, and Neptune. Radio detections of lightning have been found on Uranus from 900 KHz–40 MHz using Voyager (Zarka & Pedersen 1986) and on Saturn from 2–30 MHz using Voyager, Cassini, and UTR-2 (Zarka et al. 2004). Tenative detections of Neptune lightning from 20-30 MHz were observed by Voyager 2 (Kaiser et al. 1991), but they remain unconfirmed. Lightning radio emissions from Venus (2-30 MHz) and Mars (20-30 MHz) are also predicted to occur, but have not been observed (Zarka et al. 2008). Despite subsequent attempts using LOFAR and NenuFAR, the emissions from Saturn and Uranus have not been detected again, likely due to Earth's ionosphere and low-cadence observations. Likewise, searches for

---

[4] e.g., with the MWA and LOFAR operating at 80–300 MHz, Fallows et al. (2016) and Kaplan et al. (2015)

[5] Auroral radio emissions from Earth, Saturn, Uranus, and Neptune have all been detected but the observed frequencies are all below 1 MHz (Zarka 1998).

lightning on all the solar system planets are ongoing at NenuFAR. LFT3 is unqiue as it would allow for a relatively long-term observing campaign with no RFI. A confirmed re-detection or new discovery would carry significant implications for understanding planetary atmospheres, magnetospheres, and the general nature of the weather on planets in the outer Solar System.

System Implications: Dynamic spectra in Stokes parameters I and V with high time resolution (e.g., millisecond to a few seconds) would enable the characterization of emission morphology and polarization. Known radio flux densities from outer Solar System planets span a wide range, from $\sim$100 Jy (Uranus lightning; Zarka & Pedersen 1986) to $\sim$1000 Jy (Saturn lightning; Zarka et al. 2004), and up to MJy levels for Jupiter (Zarka 1998; Zhang et al. 1992; Zarka et al. 2004). Emission is typically concentrated between 0.1–40 MHz, a range that lies mainly below the Earth's ionospheric cutoff. The emissions associated with lightning are expected to have burst durations of seconds to minutes (Zarka & Pedersen 1986), requiring longer integration times and high spectral resolution (e.g., $\leq$100 kHz). A bandwidth covering at least 0.1–30 MHz is necessary to capture the full spectral envelope of lightning radio emissions. Additionally, dual-polarization capability is critical for distinguishing between thermal and non-thermal processes and identifying strongly polarized bursts.

2.2.3. *Exoplanet auroral radio emission*

Exoplanets with and without a magnetic field are expected to behave and evolve very differently. Therefore, there is great need to directly constrain these fields to holistically understand the properties of exoplanets. To begin with, knowledge of a planetary magnetic field can provide robust constraints on the interior structure of a planet, including its composition and thermal processes (Grießmeier 2015; Brain et al. 2024). Historically, initial insights into the interior structure of the Solar System's gas giants were derived from the understanding that they possess magnetic fields (Hubbard & Smoluchowski 1973). Furthermore, planetary magnetic fields will also affect (either enhancing or suppressing) atmospheric escape (Grießmeier 2015; Zarka 2018; Lazio et al. 2019; Egan et al. 2019; Brain et al. 2024), atmospheric dynamics and evolution (Perna et al. 2010; Beltz et al. 2023), and planetary formation (Lovelace et al. 2008; Batygin 2018; Jia et al. 2023). Ohmic dissipation could also be one of the main factors contributing to the anomalously large radii of hot Jupiters (Perna et al. 2010; Batygin & Stevenson 2010; Thorngren & Fortney 2018), one of the longest-standing mysteries in exoplanet science. Finally, magnetic fields could potentially play a crucial role in sustaining the habitability of Earth-like exoplanets by providing protection against cosmic rays (Grießmeier et al. 2015; exs 2018; Shahar et al. 2019) and aiding in understanding atmospheric escape mechanisms (Lazio et al. 2019; Zarka 2018; Kopparapu et al. 2020). Likewise, studying terrestrial magnetic fields can offer insight into other aspects of the planet that could influence its habitability, such as the presence of tectonic plates or the size of the core (Shahar et al. 2019; Kopparapu et al. 2020).

Despite decades of effort, the direct detection of magnetic fields on exoplanets has remained elusive (Grießmeier 2015; Brain et al. 2024). There are many methods proposed to constrain the magnetic fields of exoplanets. Auroral radio observations, analogous to auroral radio emissions by solar system planets, are among the best methods to detect exoplanetary magnetic fields (Zarka 2007; Zarka et al. 2015; Grießmeier 2015; Brain et al. 2024), as many of the other methods are prone to false positives (Grießmeier 2015; Turner et al. 2016; Route 2019). This radio emission is predicted to be entirely driven by the stellar wind (Zarka 2007). Therefore, the radio flux densities of exoplanets in close-in orbits are predicted to be orders of magnitude higher than Jupiter's radio flux density (Grießmeier et al. 2007; Grießmeier 2017) and thus potentially detectable with modern low-frequency radio telescopes (Zarka et al. 2015; Grießmeier 2017; Turner et al. 2019). Recently, the first tentative detection of an exoplanet, the hot Jupiter τ Boo b, in the

radio was reported from LOFAR (Turner et al. 2021). Follow-up radio observations to confirm this detection of τ Boo b are underway and so far have not redetected the exoplanet (Turner et al. 2023, 2024; Cordun et al. 2025). Also, new observations from NenuFAR have found tentative hints of emission from another hot Jupiter system, HD 189733 (Zhang et al. 2025a). A large-scale exoplanet survey with NenuFAR is currently ongoing. However, many of these systems predicted magnetic field strength place it below the ionospheric cutoff.

The search for exoplanets with LFT3 would be unique and would greatly benefit the field. To start with, there has never been an exoplanet radio search between 1-10 MHz (with the exception of the upcoming LuSEE-Night mission with which LFT3 has the opportunity to collaborate). Likewise, the planets that can be studied in this frequency range are smaller than Jupiter and thus cannot be studied from the ground. Although individual bursts from an exoplanet cannot be seen with LFT3, several key aspects of the emission will allow for stacking of observations. Exoplanetary radio emission occurs over long time scales (minutes to hours) and large bandwidths (10s of MHz), and the emission is periodic (for tidally locked planets the emission beam will be pointed towards the observer during the same part of the orbit) and circularly polarized (Zarka 2007). Therefore, we would be able to stack the entire dataset together to search for these exoplanet signals. This could be done by using a Lomb–Scargle periodogram, as recently verified on Jupiter observations from NenuFAR (Louis et al. 2025), or similar techniques. For close-in hot exoplanets, we can observe $\sim$50-100 orbits over the length of the nominal mission. Studying the radio-loud exoplanets found by NenuFAR and LOFAR (e.g. τ Boo, HD 189733) would allow us to verify this technique and enable the exploration of the outer parts of the magnetosphere that are not accessible from the ground. This study would place important constraints on the dynamo modeling, since this parameter space has never been explored before. Regardless of any detections, the science and technology lessons learned from LFT3 will help us better plan for larger radio telescopes (e.g., FARSIDE; Burns 2021) on the Moon going forward.

System Implications: The exoplanet auroral emission is predicted to peak in LFT3's Low-band (1-10 MHz) for a handful of nearby exoplanets (Grießmeier 2017). As the emission is predicted to be highly circularly polarized, only Stokes-V is needed. Previous detections from the τ Boo and HD 189733 systems range from 100's mJy to $\sim$2 Jy for individual bursts (Turner et al. 2023; Zhang et al. 2025a). Flux predictions for some planets in the 1-10 MHz frequency range extend to $\sim$100 Jy for individual bursts (Grießmeier 2017). Therefore, exoplanets may only be obsevable only by binning over large time-scales ($\sim$10s hours) and large bandwidths ($\sim$10s of MHz) and searching through the entire dataset together. It is worth noting that the theoretical flux predictions for exoplanets vary by orders of magnitude between different groups (Lazio et al. 2004; Lynch et al. 2018; Grießmeier 2017). Therefore, only observations can help constrain these models and narrowdown their applicability. LFT3's low-band observations are complementary to ongoing ground-based searches, as LFT3 will probe different planet types.

2.2.4. *Radio-bright Stars and Ultra Cool Dwarfs*

Radio stars, which are often young, magnetically active stars, provide insight into stellar magnetic activity, star formation, and the early stages of stellar evolution. Observations from a farside lunar telescope could reveal details about the mechanisms driving their radio flux (e.g. flares, CMEs) and their impact on the surrounding stellar environment. Radio-bright stars can also be used as a means of studying star-exoplanet interactions (Callingham et al. 2024). Specifically, studying radio flare stars also has implications for exoplanetary science, as the intense radiation from these flares can affect the habitability of orbiting exoplanets. A farside lunar telescope lends itself to assess the radiation environment of these planets, contributing to

our understanding of exoplanet habitability based on the low frequency window observed and the unique lack of RFI there.

Observing these stars, especially at low frequencies (≤ 300 MHz), allows us to probe stellar and planetary plasma environments. Coronal Mass Ejections (CMEs) have a low-frequency burst component in which information about the kinematics of plasma can be deduced (Villadsen & Hallinan 2019). The incident solar wind is also the primary driving force of auroral emission on magnetized planets. Radio emission from stars is typically produced through CMEs, observed phenomenologically in the Sun as type II and III solar bursts. They are also very radio-loud stars like CR Draconis peaking at 200 mJy at low frequencies (Callingham et al. 2021) making their detection a viable science goal of LFT3.

Much time has also been spent observing Ultracool Dwarfs (UCDs, spectral type M7), as they provide a good analogue to the Jovian system. This provides valuable insights into the formation and atmospheric processes of both systems. Moreover, such comparative studies contribute significantly to understanding planetary evolution and diversity beyond our immediate neighborhood. Recent detection of radiation belts around a UCD further supports the analogy to Jupiter, since radiation belts are a key characteristic of Jupiter's magnetosphere (Kao et al. 2023). UCDs, being intermediate in mass between stars and planets, serve as a bridge to understanding exoplanet detection. The discovery of bursting radio emission from a brown dwarf and subsequent detections in UCDs indicate departures from established stellar coronal/flaring relationships. Radio bursts from UCDs can exhibit periodic timing (Hallinan et al. 2006) along with strong circular polarization and high brightness temperatures, suggesting the involvement of the ECM process in generating radio emission. Despite a significant amount of gigahertz-frequency radio searches, the detection rates for UCD radio emissions remain stubbornly low at around 10% overall at higher frequencies (Lynch et al. 2016). Given that LFT3 will observe unique frequencies below 300 MHz, it can probe the magnetic field strengths higher in the magnetosphere of UCDs, offering significant insight into field geometry and strength not accessible at higher GHz frequencies.

It has also been suggested that exoplanetary magnetic fields can be studied using magnetic star-planet interactions (SPI) in the form of planet-induced radio emission (Cuntz et al. 2000; Lanza 2009; Callingham et al. 2024). Some hints are starting to emerge about SPI radio emission. This type of behavior has been confirmed between two magnetized stars in the T Tauri binary DQ Tau using radio bursts (Salter et al. 2008). Recently, (Ilin & Poppenhaeger 2022; Ilin et al. 2024) examined both *TESS* and *Kepler* data of all exoplanetary systems and found hints of a tentative correlation between flares of the star and its hot Jupiter HIP 67522 b. HIP 67522 is also detected in the radio at GHz frequencies. In the radio, coherent radio bursts on the M dwarf YZ Ceti, which hosts a compact system of terrestrial planets, were observed from 2–4 GHz on the *VLA* (Pineda & Villadsen 2023) and 550–900 MHz with the *uGMRT* (Trigilio et al. 2023). Confirmation is still needed. These observations hint at an enhancement of detected bursts at specific orbital phases of the innermost Earth-like planet, YZ Ceti b, and modeling suggests that the magnetic field of the planet could be constrained with these observations (Pineda & Villadsen 2023; Trigilio et al. 2023). A large-scale survey may find new SPI radio emission from nearby planet-hosting stars. The medium and high bands will be useful to search for star-planet interactions.

System Implications: As mentioned, radio-loud stars are on the scale of tens of mJy at lower frequencies (Driessen et al. 2024). This puts nearby flare stars well within the realms of detection. As in the other science cases, LFT3 allows observations in previously contaminated or unreachable frequencies, with the FM and sub 30 MHz bands being of particular interest for monitoring already known bright sources (Callingham et al. 2024). Time resolution of ≤ 100 ms and spectral resolution of ~ 0.1–0.5 MHz would enable

the detection and classification of coherent bursts, including ECMI-driven emission. Dual-polarization capability will be important to detect and analyze strongly circularly polarized bursts, which are diagnostic of magnetic field geometry and strength in stellar objects.

2.2.5. *Pulsars*

Pulsars are highly magnetized rotating neutron stars that emit beams of electromagnetic radiation from their poles, analogous to the rotating light of a lighthouse (Lorimer & Kramer 2004). Pulsars serve as precise cosmic clocks, providing insight into the solar wind, interstellar medium, gravitational waves, and the fundamental physics of matter under extreme conditions (Susarla et al. 2024; EPTA Collaboration et al. 2023; Reardon et al. 2023; Agazie et al. 2023; Basu et al. 2025). Pulsars are theorized to spin rapidly when they are created, but their rotation slows over time due to the combined braking effects of electromagnetic radiation, pulsar wind, and possibly gravitational wave emission (Archibald et al. 2016). Using coherent dynamic spectra, sensitivity to weak pulses can be improved and frequency and time resolution can be adjusted to decrease the effects of dispersion measure smearing (Cordes & McLaughlin 2003). Figure 8 shows the *average* radio pseudo-luminosity values for the pulsar population; individual pulses can, however, extend several orders of magnitude higher (Karuppusamy et al. 2010). LFT3 will perform single-pulse searches in order to detect the brightest subset of pulses.

Broadband studies of pulsars allow for a study of their emission physics and surrounding material, where the lower frequencies are sensitive to emission closer to the pulsar surface (Hassall et al. 2012). With ground-based radio telescopes, the ionosphere creates challenges, especially in weaker pulsars and those that have a spectral turn-over between 100–200 MHz (Stappers et al. 2011; Jankowski et al. 2018). By moving the radio telescope off Earth, circumventing the ionospheric cut-off, which is typically around 30 MHz but can be higher, a new window of study for pulsar emission physics is opened. One of the lowest-frequency pulsar detections made to date has been with the Low Frequency Array (van Haarlem et al. 2013) detecting emission down to 15 MHz with favorable ionospheric conditions (Kondratiev 2013).

System Implications: Beamformed data products are highly valuable for discovering a wide range of transient events, with pulsars being one of the potential beneficiaries. LFT3 will provide extensive sky coverage, especially at lower frequencies; however, this comes with a reduced effective area (A_{eff}) and an increased sky temperature (T_{sky}), which lowers the overall sensitivity. Consequently, the pulsar candidates identified by LFT3 will likely be giant pulses; this is due to the luminosity distribution and pulse amplitude distributions of the Galactic pulsar population (Burke-Spolaor et al. 2012; Keane 2013; Levin et al. 2013; Zhang et al. 2024; Dang et al. 2025). For some pulsars, with narrow pulse amplitude distributions, a periodicity-based search could yield detections based on the average flux densities. In Figure 9 we show the distribution of known pulsars potentially detectable by LFT3 with 10-hour coherently combined integrations, assuming flux densities reported in the ATNF Pulsar Catalogue (Manchester et al. 2005).

2.2.6. *Fast Radio Bursts*

Fast Radio Bursts (FRBs) are intense, millisecond-duration radio pulses originating from extragalactic sources. Although Galactic magnetars have been shown to exhibit similar FRB-like emission (Bochenek et al. 2020; CHIME/FRB Collaboration et al. 2020), the exact progenitors and emission mechanisms are still unknown, but the consensus is that they involve emission from neutron stars (Caleb & Keane 2021). Some bursts are observed from stellar environments which show evidence for recent star-forming activity, e.g. Piro et al. (2021). The stellar environments of other sources such as FRB 20200120E suggest that FRB
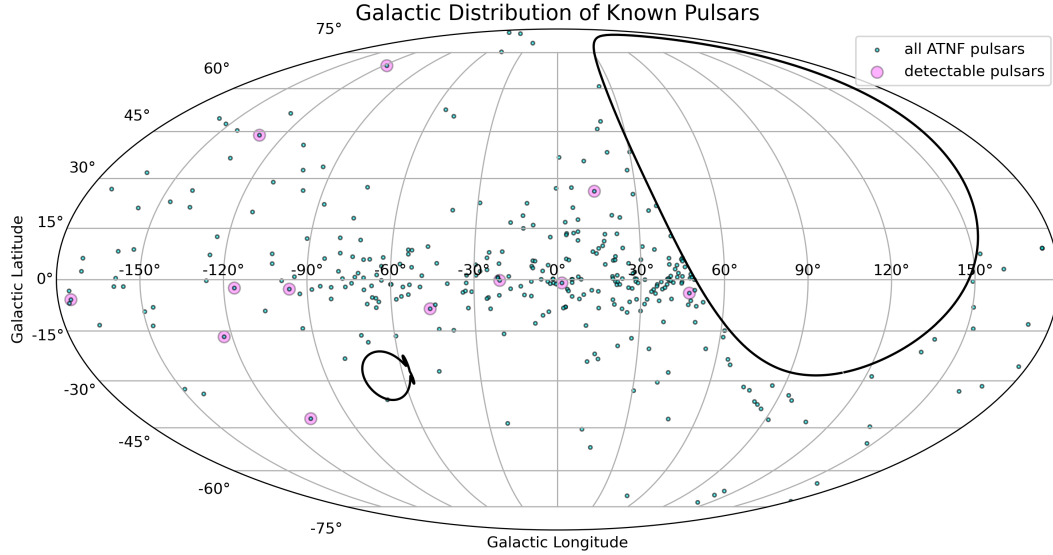
Figure 9: Distribution of pulsars detectable by LFT3 in 10 hours of observing at 400 MHz (image borrowed from Prabu et al. 2025a).

progenitors may emit bursts long after star formation activity (Kirsten et al. 2022) has ended, providing evidence for multiple formation channels.

The Canadian Hydrogen Intensity Mapping Experiment (CHIME) telescope is currently the world leader for detecting new Fast Radio Bursts with its $200\,\text{deg}^2$ field-of-view and observing frequency of 400–800 MHz, and outrigger stations for burst localization (Leung et al. 2021; Lanman et al. 2024).

A low-frequency lunar telescope, capable of high-time-resolution observations, could greatly advance our understanding of fast radio bursts, as their low-frequency emission properties are a clear factor in understanding the source populations. LFT3, supplemented by wide field-of-view ground stations on Earth could be used to co-observe to enable microarcsecond localization of the brightest FRBs, something which would be of unprecedented scientific value (see e.g. Nimmo et al. 2023). Observing beyond RFI and the ionosphere, and taking advantage of the clean FM band, may provide a key understanding to unlock the true nature and originating source of emission.

Low-frequency observations of FRBs are crucial for understanding their propagation through the intergalactic medium, potentially unveiling the distribution of baryonic matter and offering clues about the emission mechanism and source plasma environments. LOFAR observations of FRB 20180916 have revealed potential evidence for the interaction between a neutron star and its binary companion by observing bursts to 100 MHz (Pleunis et al. 2021).

System Implications: Detection of FRBs at low frequencies requires high time resolution ($\leq 1\,\text{ms}$) and sufficient spectral resolution (~ 0.1–$0.5\,\text{MHz}$) to resolve dispersion sweeps and intrinsic burst structures. While most FRBs peak between 400–800 MHz, several have been observed down to $\sim 100\,\text{MHz}$, with flux densities ranging from ~ 0.1 to hundreds of Jy (Pleunis et al. 2021). The dual polarization capability and dynamic spectra in Stokes parameters I and V will support burst characterization. Observations in the sub-100 MHz range, inaccessible from Earth, may uncover a suppressed or scattered FRB population and place limits on free-free absorption and propagation effects. LFT3's large field of view and ability to co-

observe with ground-based arrays would also enhance the chance of real-time detection and subarcsecond localization. In order to demonstrate LFT3's capacity to detect FRB-like signals, in Figure 10 we show the number of CHIME FRBs detectable by LFT3.
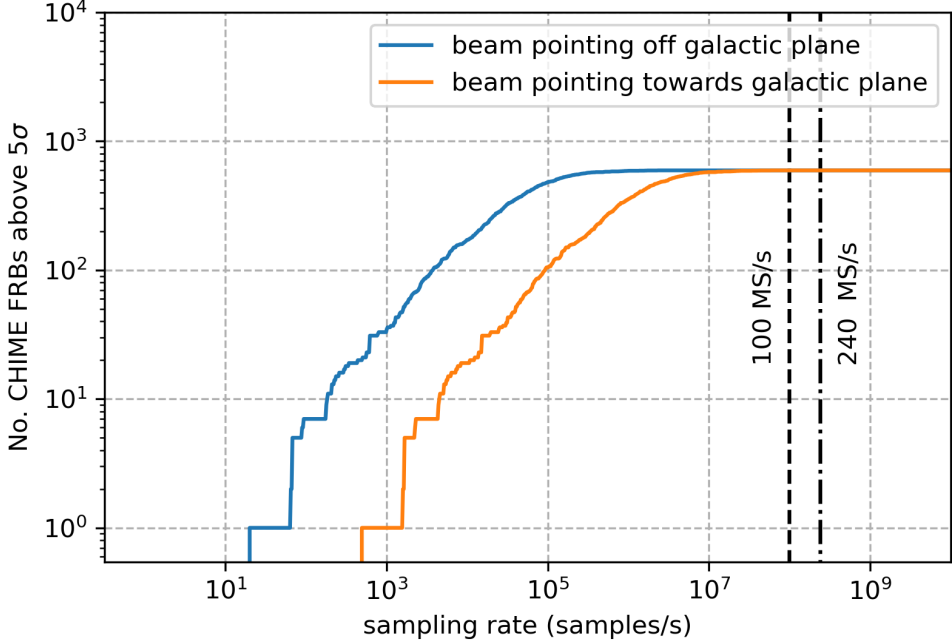

Figure 10: Number of CHIME FRBs detectable by LFT3, as function of sampling rate. We show two different lines for Galactic and off Galactic pointings (image borrowed from Prabu et al. 2025a). Note that CHIME performed these detections by observing the sky for orders of magnitude more duration than the life of the proposed LFT3 mission. The objective of the plot is to show that LFT3 is well suited to perform serendipitous FRB discoveries (by showing that most of CHIME FRBs are detectable by LFT3), the offchance that such an event where to happen within the FOV of the instrument during its mission life.

2.2.7. *Long-Period Transients*

Galactic long-period radio transients represent a burgeoning new subclass of transients. Distinguished by their exceptionally long periods, minute-long pulse duration, and low-frequency emission. The prototypical example is GLEAM-X J162759.5-523504.3 (Hurley-Walker et al. 2022). This object exhibits a period of 18.18 minutes and a pulse duration of ~ 1 minute at 100–200 MHz. The measured DM for this source was ~ 57 pc cm^{-3} indicating a Galactic origin. The distribution of pulses seen from this source are orders of magnitude larger (30–60 s) than that of FRBs and have fluxes of 5–40 Jy. This makes their discovery and cataloging one of the most feasible and impactful science goals of LFT3 (see Fig. 8). The emission is also highly linearly polarized (90%) with a spectral index of ~ 1.2, suggesting a strongly magnetized engine (Men et al. 2025). Subsequent surveys have revealed more of these objects with periods ranging from minutes to hours (Hurley-Walker et al. 2024). In particular, they show low dispersion measures ($\lesssim$ few 10^2 pc cm^{-3}) which make them relatively easy to distinguish from when observing at low frequencies. They sources are not exceedingly rare and harbor many open questions yet to be fully explored.

LFT3 presents a unique opportunity to advance this field while still in its infancy. As previously discussed, having broadband observations of these sources in an RFI pristine environment will give further insight into these objects. Such observations could reveal whether these ultralong-period objects exhibit even longer-wavelength emission, test how their spectra evolve, and potentially catch new transients with ultralow dispersion measures in the local Galaxy at these ultra-low frequencies.

System Implications: Long-period transients, with pulse durations of 30–60 s and peak flux densities ranging from 5–40 Jy at 100–200 MHz (Hurley-Walker et al. 2022), are well within the detection capabilities of LFT3. Observations should include dual-polarization data to capture the high linear polarization fraction ($\sim 90\%$) and circular emission (Bloot et al. 2025), with a spectral resolution of 0.1—- 0.5 MHz and a time resolution on the order of 1–5 s to resolve burst profiles while preserving sensitivity to slow periodicity. The observed low dispersion measures ($\lesssim 200\,\mathrm{pc\,cm^{-3}}$) reduce computational demands for de-dispersion, enabling efficient real-time searches.

2.3. *Spectral Lines*

Radio frequency interference has a significant impact when studying Galactic and extragalactic chemistry, especially in the frequency range around 1 GHz (e.g. Liang et al. 2023). This is due to an increasingly cluttered frequency band of intense signals from anthropogenic RFI, often leaking into protected radio astronomy bands. This impacts our ability to study the chemistry, kinematics, and age of astronomical objects through the spectral properties of atoms and molecules. Therefore, we must look to more creative ways of observing the Galaxy to study the dynamical motions and slow changes that are happening over the life-spans of stars and galaxies, which are critical aspects for understanding their evolution.

2.3.1. *Extra-galactic HI*

Hydrogen is the most prominent element in the Universe and the neutral hydrogen (HI) line at 21 cm (1.420 GHz) is one of the most prominent diagnostic lines used in radio astronomy. From testing models of the early Universe (i.e. Meiksin 2002) to tracing the spiral arms of our Galaxy (HI4PI Collaboration et al. 2016), HI is an important line for understanding motions and dynamics (i.e. Pingel et al. 2022). However, on Earth, even though the spectral region around the 1.42 GHz emission is protected and reserved for radio astronomy, the spectral region around the line is heavily polluted with RFI and LFT3 could augment ground-based surveys (i.e. Bhat et al. 2005; Rhee et al. 2023. This makes it challenging to study galaxies within our local Universe and beyond.

The neutral hydrogen line, observed at 1.42 GHz within our Galaxy, shifts to lower frequencies as $(1 + z)^{-1}$ as a function of the distance to the galaxy at redshift z due to cosmic expansion. For galaxies at cosmological distances, there will be many galaxies in each beam, and we measure their aggregate emission as a function of redshift. This is known as the intensity mapping technique. Although there were several proof-of-principle measurements on the ground (Paul et al. 2023), this remains a challenging technique due to foregrounds that are many orders of magnitude brighter. The unique gain stability and RFI cleanliness offered by the lunar farside might offer a novel handle on controlling the foreground emission.

System Implications: For this work, the data product would need to be a time-averaged power spectrum of beamformed targets or an incoherent sum. A spectral resolution of 100 kHz would be sufficient due to Doppler broadening of the 21 cm signal.

2.3.2. *Radio Recombination Lines*

The diffuse cold neutral medium (CNM; $T_s < 100\,\mathrm{K}$) is an important component of the interstellar medium (ISM). To date, this gas has been studied primarily using the 21 cm HI line in absorption (Dickey & Lockman 1990). A powerful and complementary probe of the conditions in the neutral ISM is provided by the cold radio recombination lines (CRRLs) that arise in this ionized gas. The low ionization potential of carbon atoms (11.4 eV) allows them to be ionized by far-UV radiation, leading to the subsequent production of CRRLs when free electrons recombine with carbon ions. CRRLs at low radio frequencies (< 1.5 GHz) have been detected in the Galactic plane in both emission and absorption with a number of telescopes (e.g. Kantharia & Anantharamaiah 2001; Salas et al. 2019; Anderson et al. 2021). The presence of radio recombination lines can impact the interpretation of global cosmic dawn measurements (Vydula et al. 2024).

At large n-bound states, observed at frequencies less than 100 MHz, the relative populations of atomic energy levels are mainly controlled by collisional processes (Tremblay et al. 2018). These collisions drive the level populations toward thermal equilibrium with the cold gas environment (typically < 100 K), resulting in the detection of these lines in absorption against strong background continuum sources. The population becomes inverted at lower n-bound states at frequencies greater than 200 MHz, resulting in emission lines being detected (Gordon & Sorochenko 2009). In the range of 100 to 200 MHz, the conversion will take place at a frequency and intensity dependent on the temperature and density of the gas within the cloud. This means that the conversion will shift toward higher frequencies as the gas density increases. This makes CRRLs excellent pressure and temperature probes of the ionized gas regions of the ISM (Salas et al. 2019).

The ionosphere negatively impacts scientific measurements as a wavelength squared dependence, thus having a greater impact on lower-frequency observations. Observing low-frequency (< 500 MHz) CRRLs is critical to understanding the temperatures and conditions of ionized gas fronts in cold gas (Salas et al. 2018). Placing a telescope far above the ionosphere would prevent ionospheric data artifacts and extrinsic spectral line broadening, which could erroneously change the measured conditions.

System Implications: The CRRLs will change width depending on the frequency of detection and the conditions of the environment. However, a resolution of 0.5 kHz would be sufficient to study the lines across proposed frequency bands. Additionally, an initial time resolution of 8-10 seconds is sufficient, with the option to average data over longer periods to increase sensitivity so long as the source remains within the field-of-view. We do this with nonmoving dipoles with ground-based telescopes by either employing fringe tracking or by doing short time recordings, correcting for the source position, and then time-averaging the data. If the dipoles were treated as independent entities, correlated visibilities would allow for a low-resolution map of the regions where the signals are detected. Additionally, beamforming can be used in two approaches: coherent beamforming, which maximizes sensitivity for known source positions, or incoherent beamforming, which sacrifices some sensitivity for a wider field of view and is more robust when detecting strong spectral lines. Overall, a spatial resolution of one degree in the sky would allow for follow-up by ground-based telescopes, where more detail is required. The preferred output is a time-averaged power spectrum or a spectrum converted to intensity in Jy. Either way, a calibration of the flux density values will be needed.

2.3.3. *Blind search for novel spectral features*

There are several mechanisms with varying levels of speculation that could produce novel spectral features in the data. Leading among them would be interactions in the dark-matter sector Keller et al. (2025). Many of such lines could be in regions of the spectrum that are heavily impacted by the RFI or the ionosphere and could have escaped detection so far. In most models these correlate with galaxies, but in some models,

such as Dark Photon Dark Matter (An et al. 2025) they appear to correlated with the Sun. LFT3 is perfectly positioned to perform a blind search for weak new spectral features across all observed radio bands that correlate with either the Galaxy or the Sun.

Another region of study for novel spectral lines is low-frequency masers. Spectral lines below 1 GHz from certain molecules indicate non-thermal emission (Tremblay et al. 2017). However, as demonstrated for Nitric Oxide by Tremblay et al. (2020), the prominent transitions at 107 MHz are significantly impacted by RFI as it resides in the FM radio band. This is true for many of the molecules of interest that have been studied by ground-based radio telescopes (Jacob et al. 2024).

Therefore, a telescope on the moon could provide a significant benefit in understanding the gas evolution, kinematics, and chemistry of astrophysical environments, away from the influence of Earth-based RFI.

System Implications: The primary system implication is in ensuring that the complete sky data product is comprehensively searched.

2.3.4. *Cosmology*

Radio observations of red-shifted atomic hydrogen have the potential to uniquely inform our knowledge of the early Universe, from the so-called Cosmic Dark Ages over 13 billion years ago, to the formation of the first stars and black holes that reionized the Universe in its last cosmic-wide change (Fialkov et al. 2024). This is because neutral hydrogen was the dominant form of baryonic matter during this period and can be detected on the basis of its 21 cm spectral line (rest frequency 1420 MHz). Of particular interest is the rise of the astrophysical structure in the cosmic fabric beginning about 13 billion years ago. Since the relevant signal emanates from a distance of 13 giga-lightyears (Gly), it is exceedingly faint, requiring extreme sensitivity and radio-quiet conditions. Since the signal of interest is also global, a single antenna is technically sufficient. Figure 11 shows a cartoon of cosmic evolution as a function of age (top) and redshift (bottom) and maps that to the observed frequency of redshifted hydrogen (yellow line).

Due to strong emission from our Galaxy at the relevant frequencies, the sky is extremely bright, with brightness temperatures ranging from about 100 K to 10^6 K depending on frequency and location, while the signal of interest is very faint (in the milliKelvin range), hence the difficulty in making the measurement. Figure 12 shows one model of the cosmological signal strength (taken from Fialkov et al. 2024) across frequencies (and hence cosmic time). Note that the observable is the difference between the hydrogen spin temperature and the CMB temperature and may be positive or negative. Making this measurement requires extremely precise knowledge of the smooth shape of the measured spectrum and removing this as a baseline. Low-level unaccounted for RFI adds uncertainty to any measurement. Precise measurements from the RFI quiet lunar farside will be invaluable in understanding that effect.

Note that LuSEE-Night, which should launch early 2026, is similarly focussed on making measurements relevant to the global signal, with all of its inherent difficulty. LFT3 will work in collaboration with LuSEE-Night to help inform these measurements. Both missions will fly the same HF antenna, although by necessity the physical arrangements will differ. Ideally, both would operate at the same time; however, this would require LuSEE-Night to remain operating for several years. There is the possibility of using the same calibration orbiter, which is a payload delivered by LuSEE-Night. One of the primary difficulties in this measurement is the affect of the lunar regolith on the received signal, and having two nearly identical systems in close proximity may be able to uniquely inform this issue.

Although it is highly unlikely that LFT3 would have sensitivity to detect either the Dark Ages or the Epoch of Reionization signals in the monopole, in the HF it could detect excess photons in the Rayleigh-Jeans tail of the CMB spectrum, which could again put strong limits on some dark matter models (Pospelov et al.
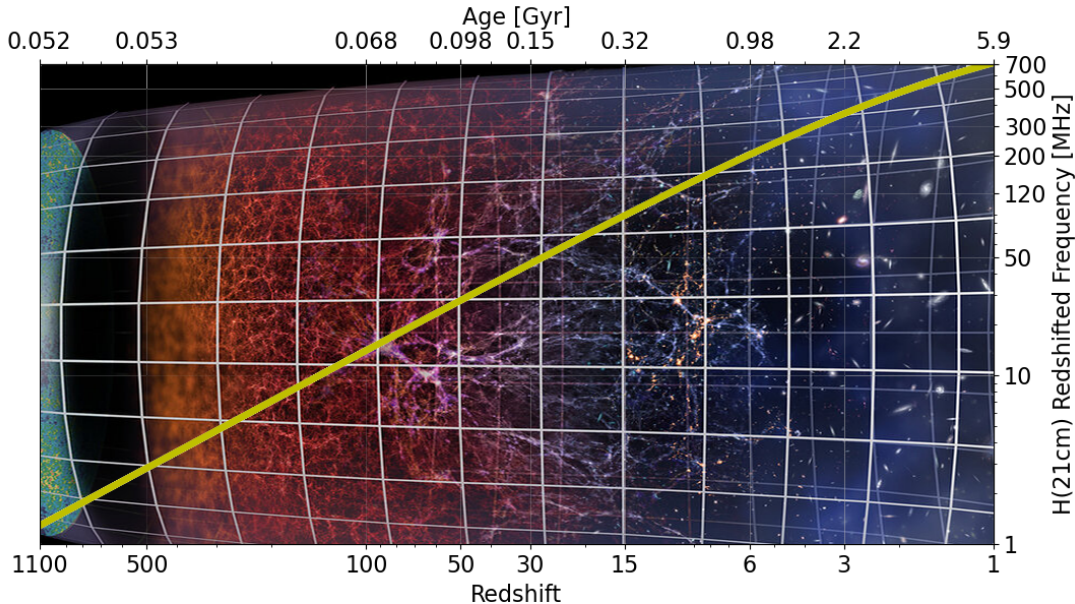
Figure 11: Cosmic evolution and observability by red-shifted hydrogen. The underlying cartoon (credit: ESO/M. Kornmesser) shows a depiction of cosmic evolution from the era of the cosmic microwave background (on the left) to the near-modern era. The top horizontal scale shows time after the Big Bang in Gyr and the bottom the associated red-shift. The yellow line and vertical axis indicate the observable frequency at that age. LFT3 has receivers across this entire range.

2018). In fact, there have been long-standing hints on excess emission in the radio sky at low frequencies (Dowell & Taylor (2018); Kogut et al. (2011)) and this is something LFT3 is uniquely positioned to test.

System Implications: The expected signal is thermal; however, that thermal profile changes with cosmic time and hence frequency, so the bandwidth and binning impact the result (see, e.g. DeBoer et al. 2017). Figure 12 shows the impact of using the 1 MHz and 10 MHz bands for this model and indicates that a few MHz bandwidth is desired[6]. Long integrations improve the sensitivity, so FOV changes on the order of minutes are the limiting factor. Given the noise of the Galactic plane, the Sun, and Jupiter, it is preferable to observe when they are all below the horizon.

2.4. *Polarization modulation by axion-like dark matter*

There has been a renewed interest in cosmology in ultralight dark matter candidates Chadha-Day et al. (2022). This framework postulates a dark matter particle with such a small mass that its de Broglie wavelength spans roughly a kiloparsec—coinciding with the scale where structure formation issues arise. This corresponds to a particle mass around $m \sim 10^{-22}$ eV. Due to this extremely low mass, achieving the observed dark matter energy density necessitates a very high number density of ULDM particles, implying that they behave collectively as a classical bosonic field, or a Bose-Einstein condensate. To stabilize this tiny mass against radiative corrections, it is typically assumed that the ULDM field is a pseudo-Goldstone boson resulting from a broken symmetry analogous to the QCD axion, which stems from the breaking of the Peccei-Quinn symmetry. Whether connected to QCD or not, such particles tend to couple to photons through non-renormalizable interactions, similar to those of axions. Particles of this kind, known as axion-

---

[6] Using as large of a bandwidth as possible is desired, since that reduces the system noise, however it can smear spectral structure.
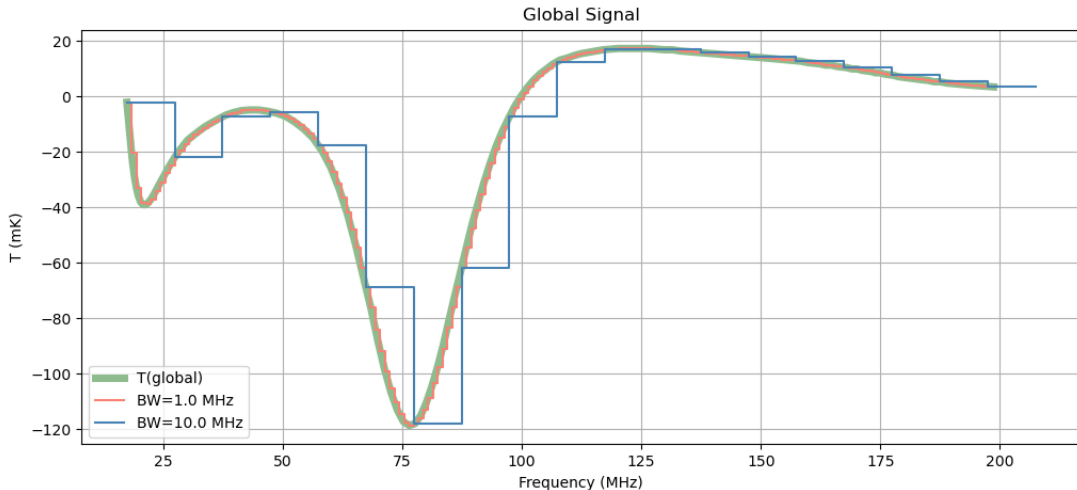
Figure 12: Global signal from the early Universe (green), which is the difference between the hydrogen spin temperature and the cosmic microwave background temperature, as taken from Fialkov et al. (2024). The blue line shows the effect of a 10 MHz measurement band, while the orange (nearly coincident with the green curve) shows the effect at 1 MHz.

like particles (ALPs), arise naturally in many beyond-the-Standard-Model scenarios, including string theory frameworks.

Coherent field oscillations of ALPs affect the propagation of electromagnetic waves through the ULDM condensate. It has been shown (Ivanov et al. 2019; Adachi et al. 2024) that the polarization angle of linearly polarized light oscillates with the same period—set by the ALP mass—which remains constant across all ALP domains in the Universe. The prediction is that the polarization angle of linearly polarized radio emission oscillates in time, which can, in principle, be detected with an instrument such as LFT3. In fact, LFT3's unique gain stability given the lunar environment and slow moon rotation allowing for long dwelling time should make it particularly sensitive to search for linearly polarizated light oscillations.

System Implications: The expected signal is weak and the polarization angle can appear to oscillate due to the gain mismatch between two polarization state channels and the variable leakage of polarization due to thermal expansion. The system should be designed to maximize the benefit of a stable environment on the lunar farside.

2.5. *Exploration of VLBI Techniques*

Very Long Baseline Interferometry (VLBI) is a powerful technique of using a large separation between antennas to obtain incredible detail of astronomical objects. This method is often used to study galaxy evolution and variability (i.e. Sheldahl et al. 2025), the precise location of sources of maser emission (i.e. Shinnaga et al. 2025), and the study of proper motion (i.e. Kumar et al. 2025). More recently, the Event Horizon Telescope (EHT; Chael et al. 2018) has used the techniques of VLBI to study black holes at the center of galaxies to provide incredible scientific detail to the regions (Event Horizon Telescope Collaboration et al. 2019).

By having a telescope on the moon with a wide range of frequency coverage, we could collaborate with ground-based facilities to test Earth-Moon VLBI methods. As the earth-based telescope has to contend with the ionosphere, joint measurements would not be available for most of the HF band (<30 MHz). However,

the other bands have significant overlap with ground-based telescopes in both the southern and northern hemispheres. Joint experiments with multiple facilities from VHF to UHF will be explored.

Additionally, the possibility will likely exist to conduct limited real-time VLBI experiments at times when the communication relay satellite can see both the spacecraft and the Earth. Given the data rates involved, this would be limited and we are looking at partnering with potential cislunar communication companies.

System Implications: To accomplish the goal, we would need to transmit time-stamped baseband data, coordinate an observation toward a shared patch of the sky, and provide precise timing clocks. We could then use a combination of conventional VLBI correlation and fridge fitting and techniques used by the EHT, which uses a more model-fitting approach to explore this technique for scientific study of the cosmos.

2.6. *Lunar Environment*

Along with advancing astronomical science, operating a telescope on the moon will also yield invaluable insights into the lunar environment and details regarding the engineering and functionality of lunar telescopes. These insights can be classified into (1) the RF environment, (2) the physical environment, and (3) the operational/engineering, as discussed below.

2.6.1. *RF Environment and Spectral Monitoring*

Although the lunar farside should be a pristine RF environment, there is the potential of some RFI from the lunar communication orbiters that will be in place, as well as spacecraft that are at distances further than the moon. There is also the potential of unknown actors emitting radio frequencies, as well as additional payloads being deployed during the LFT3 operational period, for example China's orbiting interferometer called "Discovering the Sky at the Longest Wavelengths" (DSL). As mentioned throughout, this is a time of unique change in the operating cislunar environment, and measuring a legacy spectral baseline as well as the potential increasing emergence of RFI is a key objective of this mission.

The dynamic spectra taken over the operational period and transmitted back to Earth will provide the key record of the baseline and evolving RF spectrum and LFT3 represents the **only mission** proposed to make these measurements across these bands. In addition to the dynamic spectrum, **LFT3 will catalog** *every* **measured RF event**. This will allow a unique record of the changing cislunar RF environment.

2.6.2. *Physical Environment*

The primary environmental factors of the lunar physical environment are the properties of the regolith and the extreme temperature range. The moon does have an extremely tenuous ionosphere due to solar ultraviolet radiation interacting with the lunar surface, but likely very limited impact for LFT3. These factors obviously strongly affect the operational and engineering aspects below; however, the regolith is particularly an interesting object of study. Regolith is a term used to describe any loose, unconsolidated material above the bedrock of a celestial body. The lunar regolith has effectively three different science impact components for LFT3: (1) electromagnetic, (2) structural, and (3) dust.

Electromagnetic. The electromagnetic properties of the regolith have a huge impact on the mission, particularly at the lowest frequencies and for cosmology. Understanding the lunar surface topography, conductivity, dielectric constant, emission, and reflection of radiation is the key to understanding its impact on scientific results. For the Cosmic Dark Ages science, this is arguably the most important component. The EM missions as part of NASA's Commercial Lunar Payload Service (CLPS) are essentially all leveraged to understand the lunar environment and interactions with the regolith, such as ROLSES (Hibbard et al. 2025), LuSEE-Night (Bale et al. 2023a,b) and LuSEE-Lite (Bale 2023). LFT3 would complement those

efforts and will conduct coordinated experiments with LuSEE-Night, near which LFT3 will land. Being nearby will allow studies of the same region but from a different vantage point and will provide additional information on the affects of the regolith.

Structural. LFT3 provides a unique opportunity to investigate the structure and composition of the regolith at its landing site in the farside highlands. The Moon is globally covered in inorganic regolith (also called lunar soil) about 4-5 m thick in the highlands and 10-15 m thick in the lowlands, synonymous with the lunar maria that stretch along the near side of the Moon (McKay et al. 1991). The highlands are older, more heavily cratered regions that make up the vast majority of the farside and include LFT3's landing site. As with all lunar regolith, the highland regolith has formed over billions of years from the steady erosion of bedrock by meteorite impacts. Highland regolith, based on samples examined on the near side of the Moon, has an anorthositic composition (anorthosite is an intrusive igneous rock formed when lava forms intrusions within existing rock and crystallizes) composed primarily of silicates and metal oxides.

Characterization of the regolith at LFT3's landing site will be of significant interest to engineers and planetary scientists, especially given that only two missions, Chang'e 4 (Wimmer-Schweingruber et al. 2020) and Change'e 6 (Ren et al. 2025), have successfully landed on the farside to date[7]. Such characterization will provide insights into the local regolith's physical properties. Fortunately, vital information can be obtained without dedicated sensors, using the systems already on board the lander, such as its IMU (inertial measurement unit) and touchdown sensors. For example, Firefly Aerospace's *Blue Ghost* lander, the first commercial lander to have a fully successful soft lunar landing, has footpad sensors to determine the moment when its feet contact the lunar surface (Firefly Aerospace 2025). In combination with data from the high-resolution IMU that any lander would already possess, and a detailed dynamical model of the lander itself, a relationship can be determined between the forces the lander experiences during landing and the subsidence of the regolith. An iterative multiphysics model could predict the IMU response based on the established timeline of the landing and assumed geotechnical properties of the site's regolith (based on other landing missions), such as its angle of internal friction and cohesion. Iterating this model until the predicted response converges with the measured response should produce an estimate of the actual properties of the regolith at the landing site. Constraining these properties would be of high value for any future landings in similar lunar environments, as these properties themselves constrain the design of landers and any other structures to be stably placed on the lunar surface without subsiding. Measuring the rate of the lander's temperature change throughout the lunar night, which is already required for lunar night survival, will allow estimation of the regolith's thermal conductivity, as the lander will lose heat by conduction to the lunar surface in addition to otherwise expected radiative loss.

Further low-cost sensors could greatly improve this analysis. For example, the first *Blue Ghost* mission included a set of six cameras called SCALPSS (Stereo Cameras for Lunar Plume-Surface Studies), which successfully filmed the lander's descent and touchdown from multiple angles 8 frames per second (Atkinson 2025). The images from these cameras are used to create digital elevation maps of the landing site via stereo photogrammetry. By observing how these maps change throughout the landing process, as the lander's exhaust plume scours the surface, researchers could estimate the total volume of regolith ejected, how the rate of ejection varies over time, and the depth of the removed layers (Tyrrell et al. 2022). These data, when analyzed together with a multiphysics model of the landing, could reveal how the properties of the regolith vary with depth near the surface. Characterizing plume-surface interactions, as with the SCALPSS exper-

---

[7] Chang'e 6 returned samples of the lunar farside

iment, could also help quantify the hazards to surrounding infrastructure posed by landing on unprepared lunar surfaces nearby. Even something as simple as having cameras with the lander's footpads in view could reveal their penetration depth into the regolith after landing, allowing the regolith's bearing capacity to be calculated.

Any of these low-cost measurements and analyses will be valuable for planning future missions and improving the quality of lunar simulations.

Dust. The top surface of the moon comprises a very fine dust with 20% of particles by weight having a diameter below 20 μm (Zanon et al. 2023). Lunar dust is very abrasive and becomes electrostatically charged as a result of interactions with solar wind and UV radiation. The act of landing on the moon generates copious amounts of dust that can settle on the hardware of the lander and affect performance and operations. Although electrostatically charged abrasive dust has proven destructive to mechanical joints and pressure seals, it has been less of a problem for RF hardware and antennas. The Chang'e 4 lander has been operational since landing on the lunar farside in 2019, with no negative effects from dust noted regarding operation of its X-band antenna, lunar penetrating radar (which has channels at 60 and 500 MHz), or low-frequency radio spectrometer (which measures in the 0.1-40 MHz range) (Jia et al. 2018).

Fortunately, proactive measures can be taken to avoid leaving the impacts of dust adherence to chance. Voyager Space successfully tested a passive "clear dust repellant coating" aboard *Blue Ghost* Mission 1, a CLPS mission, which landed on February 2, 2025 (Voyager Technologies 2025). This mission also tested NASA's electrodynamic dust shield, a low-mass system that draws 2-4 W of power to remove dust particles with electric fields using transparent indium tin oxide electrodes, which allows it to remove dust from optical sensors and camera lenses in addition to other components (Buhler et al. 2020). The dust shield has demonstrated 98% dust removal during laboratory testing, with improved performance under lunar analogue UV exposure (Wang et al. 2024) and the results of lunar systems are still pending. Various passively dust-tolerant mechanisms, including seals and bearings, are also being developed (Fritz et al. 2024).

The dust mitigation measures ultimately employed by LFT3 will help demonstrate protection of sensitive RF equipment in the lunar environment, with qualitative data on the extent and effects of dust adherence being gathered with optical imaging of the lander's instruments and RF measurements.

2.6.3. *Operational and Engineering Impact*

LFT3 will gather baseline RF spectra for the lunar farside environment, which will benefit any future farside missions that take RF measurements. The data handling procedures established to store and transmit LFT3's measured data to Earth will similarly be useful for any future farside missions, none of which can directly transmit data to Earth. As with the CLPS missions, LFT3 will help establish the relevant electromagnetic impacts of regolith on RF instruments, with special attention to impacts on high sensitivity, low frequency radio astronomy.

Data gathered by LFT3's IMU and surface contact sensors will allow for the estimation of the geotechnical properties of the local regolith, such as its cohesion, angle of internal friction, and bearing capacity. Additional low-cost cameras could stereoscopically film the descent of the lander, revealing interactions between its exhaust plume and the regolith at the surface, providing information to strengthen the analyses of the regolith's properties. Even without dedicated sensors, vital information about the regolith can be gathered for use in future lunar surface missions.

LFT3 may include a payload to assess the performance of potential lunar construction materials. A promising candidate is the biopolymer-bound soil composite (BSC), a material comparable to concrete that binds to lunar regolith using a small fraction of a biopolymer binding agent (Rosa et al. 2020). A sys-

tem is envisioned to image a set of BSC samples (made with regolith simulant) and control samples (made of conventional concrete) with a pair of stereoscopic cameras. Images taken over time will show the extent of cracking or spalling due to environmental exposure. Miniature load cells for each sample would allow for measurement of stress due to thermal expansion and contraction, allowing for calculation of their elastic modulus and any changes to their elastic behavior over time. Embedded strain gauges and thermocouples within the samples would provide additional complementary data.

The dust mitigation techniques employed by LFT3 will be relevant for future lunar surface missions, regardless of their specific purpose. Alongside the CLPS missions and other future surface missions, LFT3 will play an important role in helping engineers converge on a set of practical solutions to avoid the negative effects of lunar dust adherence.

Furthermore, techniques to survive the cold night temperatures are critical to future missions, and the techniques employed by LFT3 will further our understanding of effective mechanisms. In addition, partners will be sought to provide additional sensors or data analyses for lunar environmental characterization.

2.7. *Science Summary*

The strength of LFT3 lies in its ability to uncover the unknown while operating in a completely unprecedented environment. As the only mission with the goal of capitalizing on this unique moment in human history, LFT3 stands at the forefront of discovery. Table 1 provides a summary of the primary science objectives along with some of their system needs. Additionally, the robust design is tolerant to system issues that may arise in landing or operation, within the scope of the mission.

It is important to emphasize that any observation with LFT3, regardless of resolution, will be unique and scientifically valuable. With its high-performance design, LFT3 will leave a lasting legacy, documenting the transition of the cislunar environment, potentially discovering new phenomena, and addressing long-standing questions about known phenomena.

3. PAYLOAD AND OPERATIONS

The previous section outlined the science case for a telescope on the lunar farside and the results are summarized in Appendix A. Ideally, one would build a large and flexible observatory, and discussions for such telescopes are underway (e.g. Burns et al. 2021b, Bandyopadhyay et al. 2021). However, to take advantage of this unique opportunity for early measurements, two additional constraints inform the payload design: (1) land and operate before the end of the decade (by 2030) and (2) achieve the goals for a budget of US\$150M or less. The design is therefore structured around these additional objectives, meaning it has similar schedule and budget requirements to missions under the NASA Commercial Lunar Payload Service (CLPS) program. The lunar lander will have a diameter of approximately 4 m and a science payload mass of approximately 100 kg. One main difference from the NASA CLPS program is our ability to work with potential vendors to increase compatibility between the lander and science payload. For example, the LuSEE-Night program carries its own power system (solar panel and battery) and communication system and requires the lander to electrically passivate itself at the end of the lunar day. This simplifies lander-payload interfaces and gives LuSEE-Night full control over the RFI environment at the expense of increased payload complexity, weight, and cost. For LFT3 we want to work much closer with the vendors and rely on lander for power and communication. The primary concern is electromagnetic compatibility and the need to minimize radio frequency interference affects, which will be achieved by a combination of requirements on instrument design (syncing all clocks to precisely place power supply harmonics) and operational constraints (switching off non-essential equipment when taking science data). Table 2 summa-

Table 1: System requirements for each mission objective. Band characteristics are defined in Table 3. Science category 1 is Lunar-Exclusive Science, category 2 is Lunar-Augmented Science, and category 3 is Proof-of-Concept Science (see Figure 18).

Mission Objective	Receiver Band	Freq. Res.	Time Res.	Objects of interest	Stokes	Category
Technosignatures	HF/VHF/UHF	10Hz	1sec	catalog/blind survey	I, Q, U, V	1,2
Pulsar	HF/VHF/UHF	0.5MHz	1ms	catalog/blind survey	I	2,3
FRB Analogs	HF/VHF/UHF	0.5MHz	10ms	catalog/blind survey	I	1,2
Flare Stars	HF/VHF	0.5MHz	1sec	Gaia Stars	I, V	2
	UHF	N/A	N/A	N/A	I	3
Exoplanets	HF	10MHz	hours	Nearby exoplanets	I,V	1
Solar System	HF/VHF	100 kHz	1s	All SS Planets	I,V	2
	UHF	1 MHz	minutes		I	3
Studies of the Sun	HF/VHF	0.5MHz	1–2ms	Sun	I,V	3
	VHF	0.5MHz	1–2ms	Sun	I	3
HI Studies	HF	N/A	N/A	N/A	I	3
	VHF/UHF	1kHz	5–8sec	Radio Galaxies	I	3
RRL	HF	N/A	N/A	N/A	I	2
	VHF/UHF	0.5kHz	5–8sec	SNR, HMS[1]	I	3
Cosmology	HF/VHF	1 MHz	minutes	Non-Galactic Plane	I	2
VLBI	HF/VHF/UHF				BB	1
Lunar studies	HF/VHF/UHF	1 kHz	1s	Moon	I	1

[1]HMS=High mass star formation regions

Table 2: Payload Requirements

Parameter	Value	Notes
Span	∼4 m	This varies with vendor.
Mass	100 kg	This is the science payload mass.
Power (day)	200 W	Balancing day/night operations.
Power (night)	30 W	Included in the lander mass budget.
Comms	100 GB/month	The nominal budget includes 20 weeks of operation
Storage	20 TB	This coupled with comms and processing scopes the system.

rizes the scope of the payload that fits within the constraints. These numbers represent an evolutionary and realistic step-up from the parameters of LuSEE-Night.

A rendering of the lander is shown in Figure 13 and a schematic of the science payload is shown in Figure 14. The five antenna subsystems are summarized in Table 3. The UHF-Lo array covers most of the lander top surface with 48 dual-polarization wideband antenna elements. The array forms a fan of beams on the sky designed to cover 70% of the lunar sky over time (Fig. 15). Formed beam output signals are downconverted and sampled in a 50 MHz subband that is scanned across the array operating bandwidth.
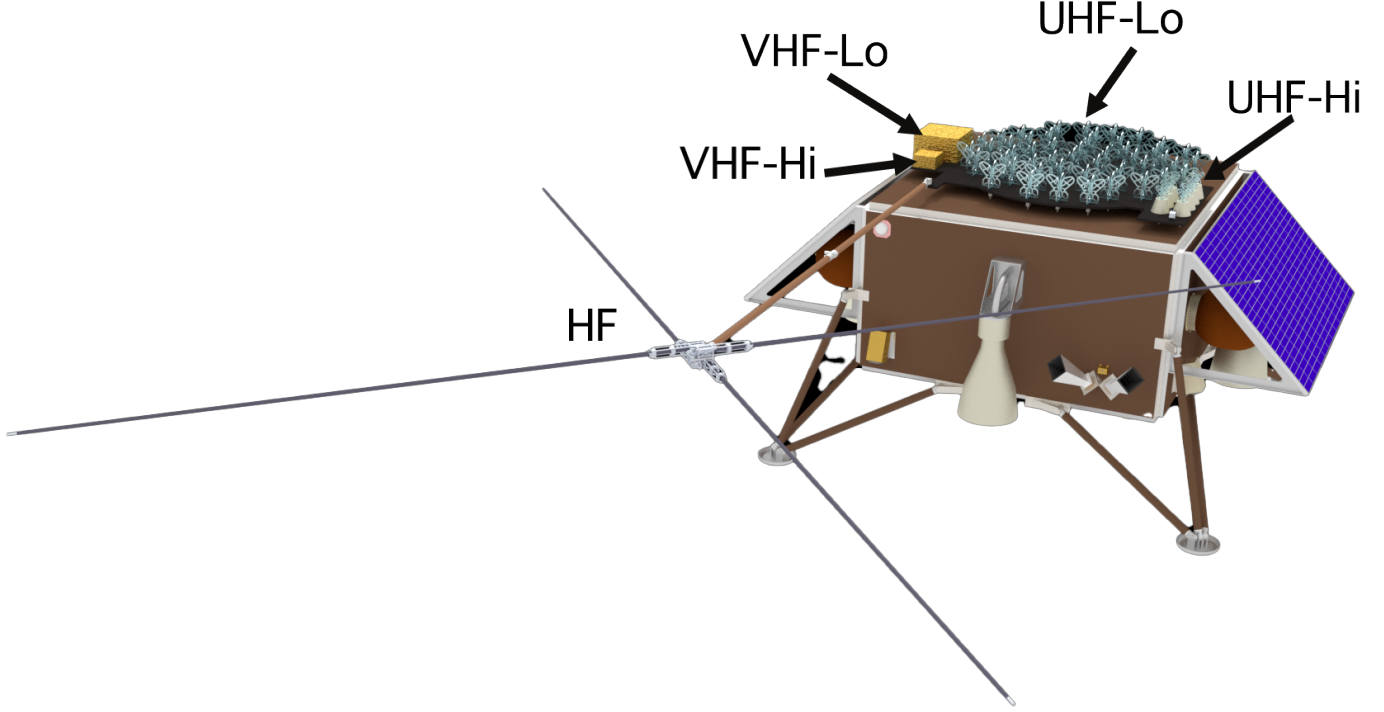
Figure 13: Rendering of the generic science lander and payload. The antennas are all located on the top deck, and the beamformer and processor are located in a thermal cavity directly below. The antenna elements are annotated per band.

Table 3: Basic system parameters of the receiver sub-system. The sensitivity is shown in Figure 3. There are a total of 16 sky-fixed dual-polarization beams, of which 8 can be observed at the same time subject to switching network constraints (see Figure 14).

Band	Freq Range	Antenna design	Beams	Beam size (degrees)
HF	1 - 50	Cross pseudo-dipole	1	$45° - 90°$
VHF-Lo	60 - 110	printed film	1	$80°$
VHF-Hi	150 - 250	printed film	1	$80°$
UHF-Lo	300 - 900	phased array (Vivaldi$\times$48)	10	$4° - 16°$
UHF-Hi	900 - 2700	phased array (Vivaldi$\times$8)	3	$20° - 60°$

Efforts are underway to see if that bandwidth can be extended. The system design has two spectrometers whose preliminary specifications are shown in Table 4.

Operational constraints have a huge impact on the observation strategy, the derived data products, and the downloaded data. The available full-day power is ~200 W, which reduces to ~30 W at night, and the expected download capacity is 100 GB/month. The expected on-board memory will be 20 TB. The beamformer and individual antennas will produce dual-linear polarizations. The spectrometer will produce pseudo-Stokes dynamic spectra of varying spectral/temporal resolutions. On an appropriate trigger, it will also produce full base-band data over the last trigger. The on-board instrument processor unit (IPU) will provide any post-processing of the dynamic spectra and coordinate memory and transmission back to Earth.
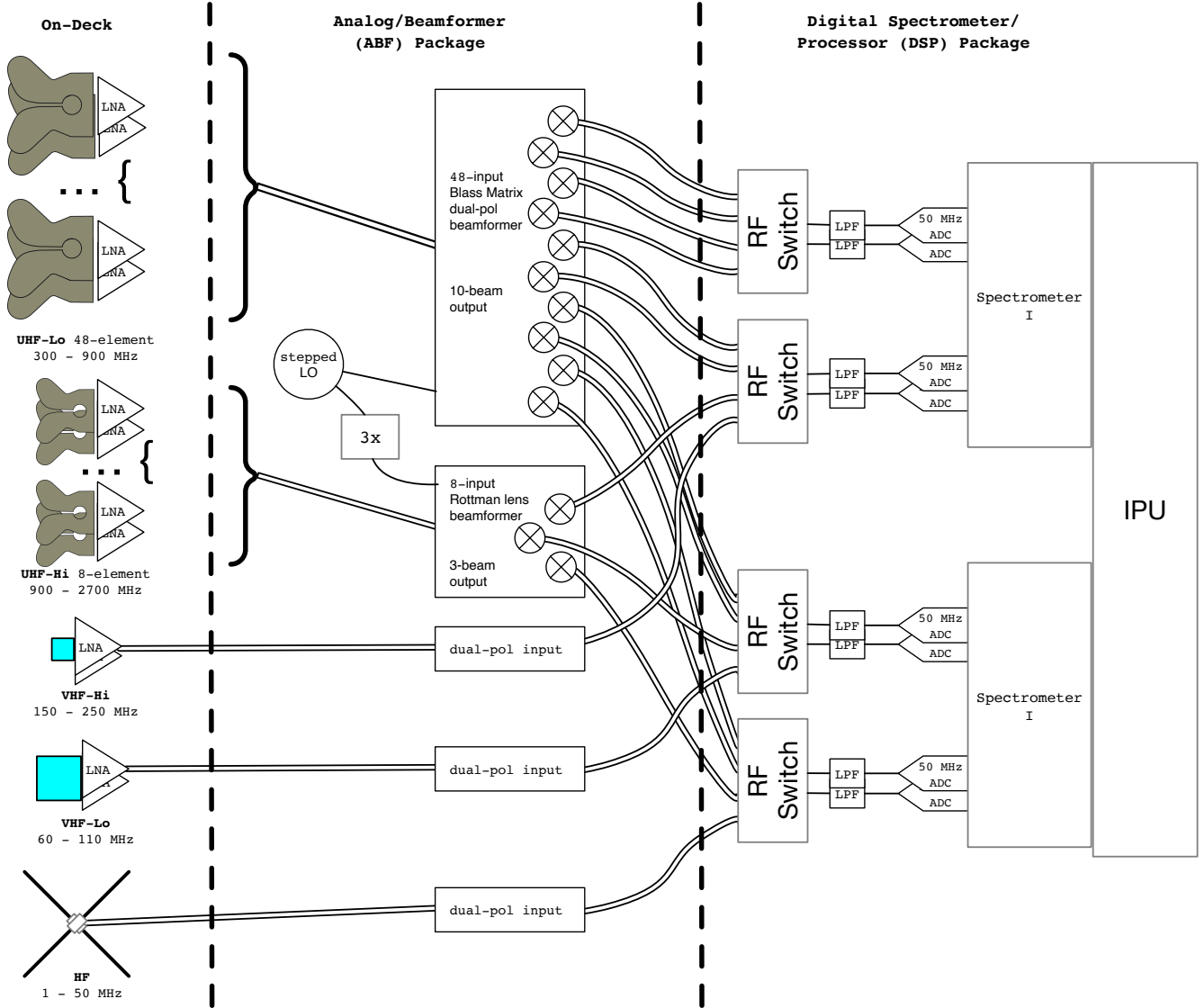
Figure 14: Block diagram of the science payload. The five bands are shown on the left. The UHF bands go into a heterodyne and beamforming system to chose the frequency sub-band and form the beams. All of the RF inputs go into RF switches before digitization and processing. The exact partitioning of the system will be addressed in the next design phase. As currently shown, there are two spectrometers for redundancy. The Instrument Processing Unit (IPU) conducts the processing and saves the data for transmission to Earth.
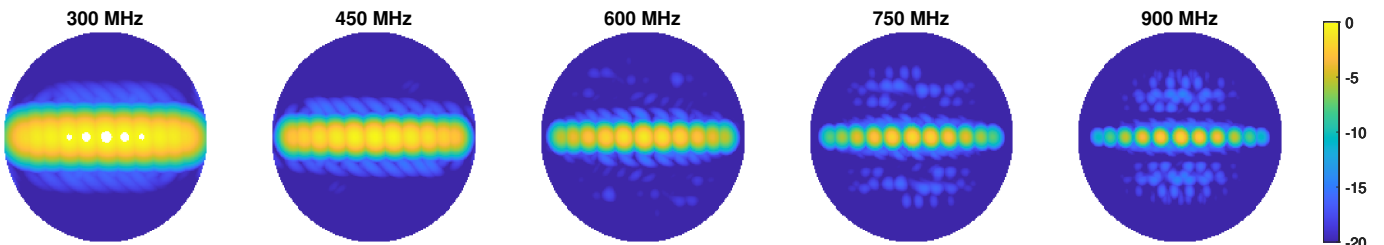
Figure 15: Midband array formed beams over frequency. Scale is aperture efficiency in dB relative to a 3 meter diameter area. Beams are centered within 11 equal intervals over a 120 degree field of view.

Table 4: Basic spectrometer parameters. LFT3 will operate two such spectrometers.

Parameter	Value
Number of input channels	8
Bandwidth	>50 MHz
Duty-cycle	100%
Correlation products	4
Spectral Channels	2^9 - 2^{22} (i.e. 512 - 4×10^6)
Polyphase filterbank taps	8
ring-buffer size	1 second
Power-consumption	<12 W
Additional capabilities	technosignature search, pulsar signal detection & folding, dedispersion, general transient detection

The communication back to Earth for data will be limited to the lunar day. The concept of operations is discussed in Section 3.2.

3.1. *Lunar Farside Location*

The lunar farside is a unique location in the solar system in that it is the only area that never faces Earth due to tidal locking. This means that it is always blocked from terrestrial and near-terrestrial radio frequency transmissions. This importance was recognized in the 1970s when the International Telecommunication Union (ITU[8] defined the Shielded Zone of the Moon (SZM) as "compris[ing] the area of the Moon's surface and an adjacent volume of space which are shielded from emissions originating within a distance of 100,000 km from the center of the Earth" (ITU 2024). This essential radio quietness will be exploited by LFT3. Figure 16 shows a projection of the lunar orbit to give a sense of scale of Earth's size, the Moon's size, the distance from Earth, and the variability of the orbit.

The landing site coordinates of 23.78930°S, 182.13737°E (Fig. 17) are well within the SZM and are also near the LuSEE-Night landing location, with which it will coordinate. In the Equatorial Farside region, lunar days and lunar nights each last approximately 14 Earth days. This results in survival temperatures ranging from 100 K to 400 K (Vasavada et al. 2012). Additionally, landing near LuSEE-Night provides a known location with recent landing experience, increasing the chance of a successful landing.

3.2. *Concept of Operations*

In this section, we outline the LFT3 science operations framework designed to efficiently support the proposed science goals by allocating appropriate mission resources —-such as observation time and downlink capacity—to each science objective. A more complete description can be found in Prabu et al. (2025a). The science goals described in this white paper are broadly grouped into three categories which correspond to the categories in Table 1: lunar-exclusive science goals, lunar-augmented science goals, and proof-of-concept science goals. Lunar-exclusive science goals include measurements uniquely enabled by the radio-quiet, ionosphere-free environment of the lunar farside—such as unambigious searches for technosignatures, detection of low DM transients, cosmology, and legacy RF surveys of the Moon's farside that will serve as a baseline before future RFI contamination. Lunar-augmented science goals build upon and

---

[8] The ITU is the international organization that handles electromagnetic emission across national boundaries.
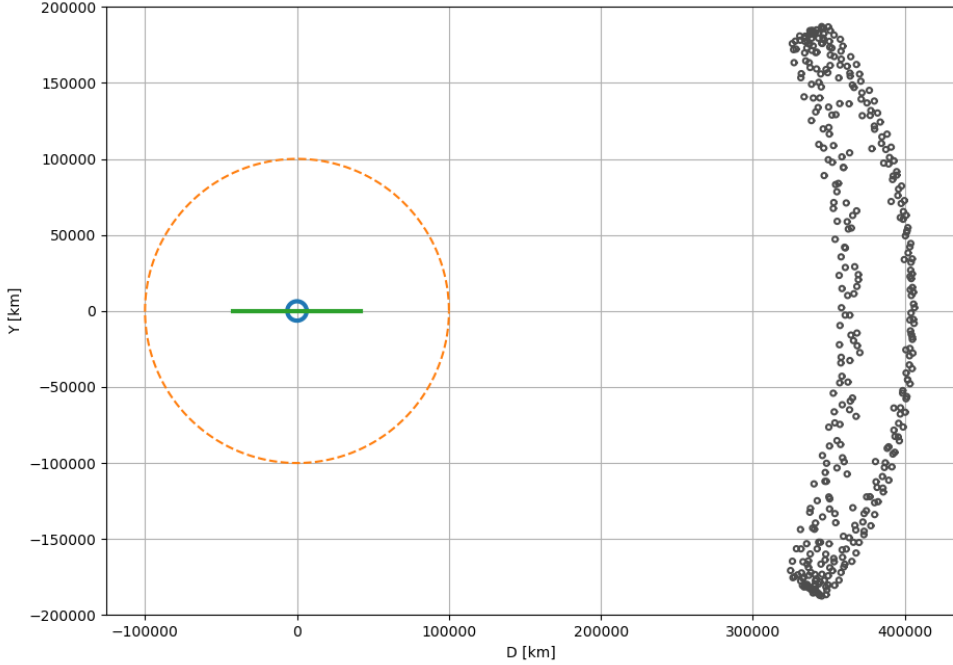
Figure 16: Projection of the lunar orbit showing the relative sizes and variability. The Earth is at the origin and the location of the Moon is shown for every day of 2028. The x-axis is the distance from the Earth and the y-axis is the distance out of the equatorial plane. The green line is the geostationary arc and the orange circle is the 100,000km SZM defining circle. The relative sizes of the Earth and Moon are to scale.

enhance Earth-based observations with additional complementary low-frequency wideband measurements, thus improving the overall scientific understanding of known astrophysical sources. Proof-of-concept science involves replicating measurements that can also be performed from Earth, with the goal of validating LFT3's scientific capabilities and calibrating its measurements against the ones from Earth-based observatories. Examples of this will be observing bright quasars, pulsars, and hydroxyl masers. A high-level categorization of all science goals into these three groups is shown in Figure 18.

All LFT3 science operations will be conducted in two distinct modes: real-time observations and targeted observations. A real-time processing pipeline will operate continuously across all observed fields, constantly looking for transients and technosignature candidates. A real-time search system that runs throughout the 20-week mission life of LFT3 maximizes our likelihood of serendipitous discoveries of transient events. Due to their persistence in the sky, all other science targets (such as pulsars, Sun, solar system planets, etc.) will be observed as the targeted observations with appropriate scheduling (such as choice of beam to process, time and frequency resolution of the output science data, frequency tuning, and number of Stokes parameters to record) as and when the target appears within LFT3's visible sky. A complete breakdown of the observing schedule for these science targets and the corresponding generated science data volume can be found in Prabu et al. (2025a).

Due to the lack of a line-of-sight link to LFT3 from Earth-based groundstations, science data products from LFT3 must be relayed to Earth through an intermediate lunar orbiting satellite. Currently, this method
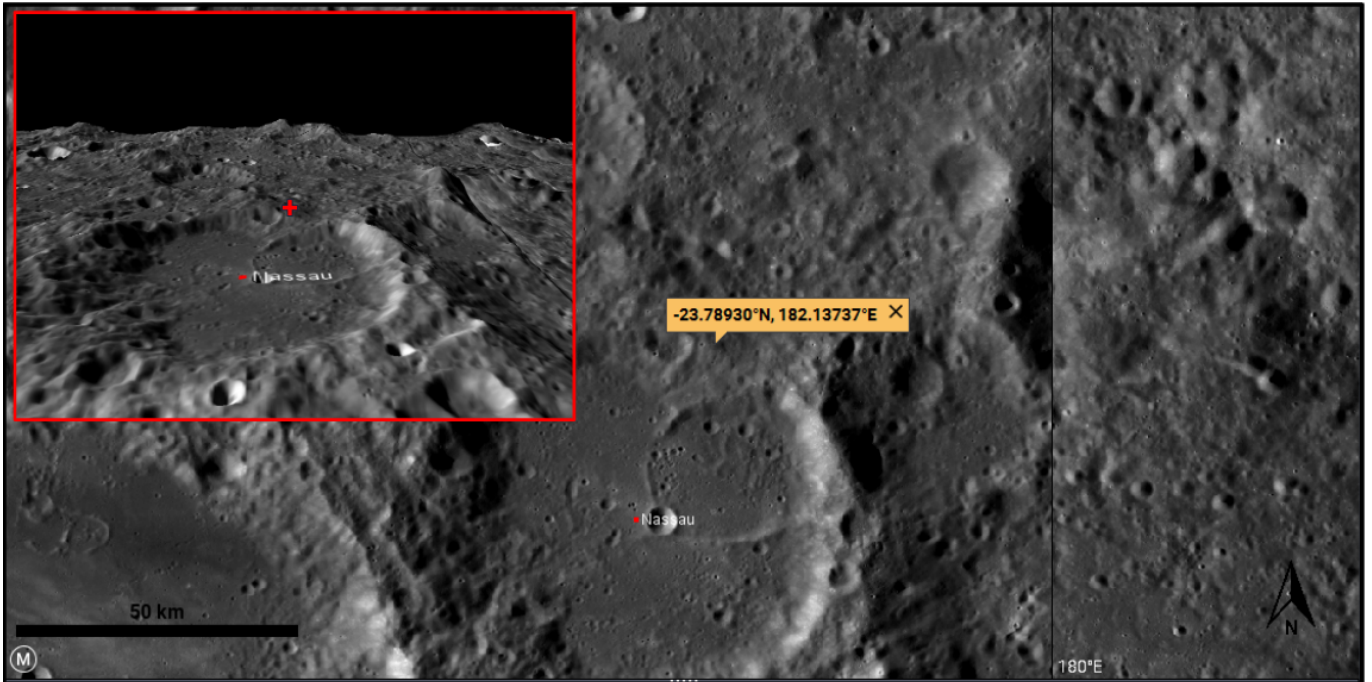
Figure 17: LFT3 Farside Landing Site - Micro View JMARS
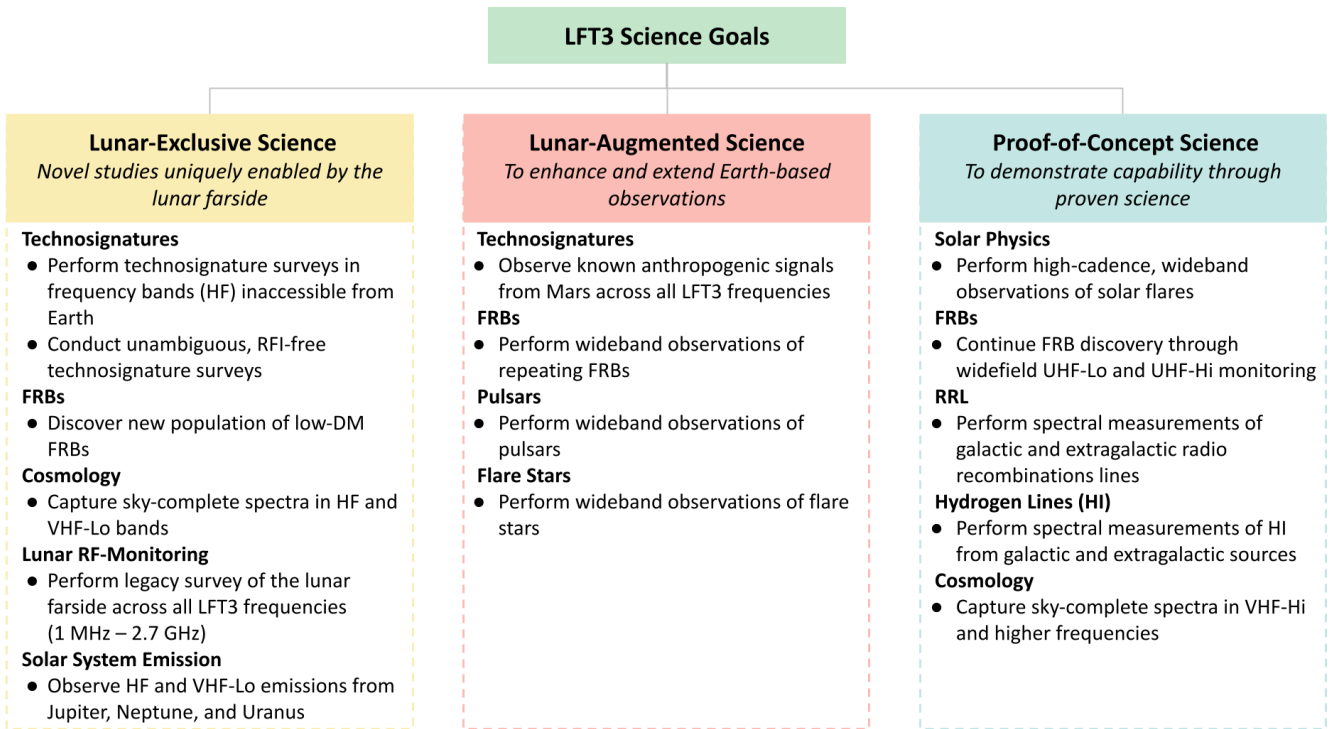
Figure 18: A high level breakdown of LFT3 science goals into lunar-exclusive science goals, lunar-augumented science goals, and proof-of-concept science goals (image borrowed from Prabu et al. (2025a).)

Table 5: Uncompressed volume of data products produced by LFT3 per lunar cycle (28 Earth days). Note that the total data generated is over the 100GB limit. The science data can be fit within the budget using data compression methods, which may potentially be lossy.

Product type	Data Volume [GB]	Total integration time
Baseband data	20	10 seconds
Dynamic spectra	255.6	336 hours
Sky-complete spectra	0.5	672 hours
Event Catalog	≤ 1	1.4×10^9 events (at 5σ)
Meta-data and housekeeping	≤ 1	-

of downlinking data back to Earth is effectively limited to 100 GB/month. Hence, to ensure optimal use of this limited data rate, we define four different science data products that will be produced by LFT3, namely, baseband data, sky-complete spectra, high-resolution dynamic spectra and event catalog (see Table 5). For high SNR transient and technosignature events seen by LFT3, 1s of baseband data (about 2GB/s) will be downlinked back to Earth. For all other targeted science observations, only high-resolution dynamic spectra (produced at a rate of $0.0004 - 50$ MB/s based on the science target being observed) are transmitted back to Earth from the LFT3 beam containing the target, and the time/frequency resolution of these dynamic spectra is dictated by the science requirements of the target. For all the fields being observed by LFT3 during its life, a coarse resolution spectra (1MHz frequency resolution and 5 minute time integrations) called the sky complete spectra are generated. This sky complete spectra maps out the complete celestial sphere seen by LFT3 during its life, and contributes towards the comology and lunar-RF monitoring studies proposed in this white paper. The payload also maintains an onboard catalog of low-SNR pulse signals in the form of an event catalog, which will be used for gathering statistics of false positives (and any underlying low-SNR astrophysical transient population) seen by the instrument.

Overall, the mission timeline aims to launch the LFT3 payload in 2028, with a high-level functional requirement for 20 weeks of operation. The high-level science traceability matrix of the mission can be found in Figure 19. The proposed science operations plan in Prabu et al. (2025a), aims to meet all mission objectives within the 20-week time frame, by allocating sufficient observation times to each of the science goals and a data management plan to download the highest priority data.

4. OTHER CONSIDERATIONS

This paper presents a science case for an instrument landing and operating from the lunar farside surface. Other possible missions obviously exist, which will be briefly discussed in the following. However, we believe that a lunar farside surface instrument possesses compelling and unique aspects such as a consistently radio-quiet environment, site stability (e.g., Burns et al. 2021a), study operational requirements when operating on the moon, and being able to design a telescope with broad frequency capabilities, all contributing to a larger understanding important for designing larger missions in the future. And, as mentioned earlier, this mission is not predicated on what might be done if one had a fairly large budget to design and build a radio telescope on Earth, but rather what could one do for an inexpensive lunar mission that advances science and our understanding of operating on the moon.

4.1. *Surface of Earth*

Although radio telescopes are often built in remote places away from dense urban areas, they are still significantly more accessible than space-based instruments. This proximity allows for large apertures, maintainable and changeable hardware, and the ability to process and transport large amounts of data. However, the disadvantages are two-fold, severe, and unmitigatable: 1) the atmosphere and ionosphere block and distort signals at many important radio frequencies of interest and 2) on- and off-world human activities cause significant radio frequency interference (RFI) that contaminates the collected data with erroneous artifacts. The first disadvantage is certainly not remediable from the Earth's surface, while the second disadvantage has previously been ameliorated by building in very remote places. But in recent decades, the construction of radio facilities in remote sites is no longer sufficient: more radio-loud technology has spread throughout the country and, recently, emissions from large satellite constellations have severely affected ground-based radio data (Zhang et al. 2025b; Grigg et al. 2025; Zhang 2025; Bassa et al. 2024). Therefore, it is no longer a simple matter to find a quiet environment on Earth – all locations imply a loss of discovery opportunity.

To combat the problem of RFI we can build telescope antennas in locations which are not in close proximity to each other. Using the very long baseline interferometry techniques (VLBI), we can then connect the telescopes through software and correlate the signals. This means that any signal that originates in the local environment would not significantly impact the final result. There are approximately six VLBI networks on Earth that are used by the scientific community. While they each offer microarcsecond scale resolution of the Universe, they suffer from significant computational challenges when correlating data from multiple sources and wide fields. This may be generalized beyond VLBI to investigate various methods of using widely-separated coherent detectors to help mitigate RFI.The use of VLBI limits RFI contamination but does not eliminate it because RFI-producing satellites can appear simultaneously within the field of view of multiple antennas. VLBI also does not change the limits of the frequency range observable from Earth because of atmospheric and ionospheric effects. However, this technique remains our best long-term path forward to deploy significant sensitivity, even with the negative discovery impact of RFI.

To combat both of these problems in other wavelengths, we now readily build telescopes on satellites, airplanes, and even the International Space Station. However, this solution ironically contributes to the problem of anthropogenic interference for radio facilities on the ground. Due to the increasing privatization and decreasing costs of space flight and launch equipment, we can now consider performing radio astronomy from non-terrestrial environments as well. However, as pointed out, the same technology is driving other activity to space as well.

4.2. *Low Earth Orbit*

Getting into Earth orbit is beneficial for low-frequency observations, although there will be some leakage through the ionosphere to space. Since the 1970s, several space-based observatories have been successfully launched into low-Earth orbits to provide unique views of the skies. Some of the most successful missions provided decades of legacy data that continue to contribute to new discoveries. Some examples include the *Hubble Space Telescope*, *Hershel Space Telescope*, and the *Chandra X-ray Observatory*. These missions were developed because of the need to leave the atmosphere of the Earth to effectively study the cosmos at their associated wavelengths (i.e. optical, infrared, and x-ray).

Although an orbiting radio astronomy telescope provides the advantage of escaping the ionosphere, increasing its scientific scope over ground-based systems, it does not create an effective barrier against anthropogenic radio signals. Although algorithms can help identify and flag some RFI, they cannot fully restore data quality. Contaminated data are often irretrievably lost, and subtle astronomical signals can be

completely masked by this interference. So, for VHF and above, there is no advantage of low Earth orbit over Earth-based sites, and orbit provide a multitude of additional challenges.

4.3. *Lunar Orbit*

Lunar orbit has some advantages: no risk of landing, no need for a relay satellite, and a decreased need for batteries. The preference is a matter of mission goals, and lunar orbit has some key disadvantages:

- potential of RFI due to necessary station-keeping activities,

- rapidly changing platform characteristics,

- RFI-quiet only for roughly 1/3 of the time,

- we don't learn about the Moon itself,

- we don't learn about operating on the Moon.

Note that the communication relay orbiters are already going to be in place by the time of LFT3 so the communications infrastructure is available, and the spacecraft will not require the higher-power and higher-frequency communications package to communicate back to Earth.

4.4. *Lunar Surface*

After landing, a farside surface telescope would be entirely stationary with respect to the Moon, simplifying its operations and making them more similar to those of a traditional Earth-based telescope than an orbital telescope. As explained before, being on the lunar farside also guarantees continuous shielding from RFI rather than the only intermittent shielding a lunar orbiting telescope would have. Lunar orbiting telescopes face an unfortunate tradeoff between RFI shielding and orbital stationkeeping complexity. Lower lunar orbits spend more of their time in the lunar farside's radio shadow, shielding them from RFI, but decay much more quickly due to lunar mass concentrations that destabilize orbits. Higher orbits can last much longer without decaying but are accordingly shielded for much shorter periods. A surface-based farside telescope would escape this trade-off entirely, as it eliminates all orbital stationkeeping requirements and would be shielded against RFI 100% of the time. Orbital station-keeping also has the potential to produce self-generated RFI. The dwell time on a patch of sky is quite long (about 30 times that of Earth), which affords better survey properties.

5. CONCLUSION

As the only proposed mission to exploit the singular opportunity for RFI-free astrophysical observations across HF, VHF, and UHF from the lunar farside, the LFT3 mission is uniquely positioned to redefine our understanding of the radio universe from this unique vantage point in space and time. In an environment quieter than even that in which the famed "Wow!" signal was detected, LFT3 offers an unprecedented chance to conduct technosignature searches with confidence and unambiguity never before possible in human history. Crucially, this opportunity is time sensitive. The lunar farside will soon face increasing RFI contamination as more missions are launched, and the timeline for the proposed LFT3 mission is uniquely aligned to capitalize on this fleeting window. Every signal detected by LFT3 in this pristine radio environment will have an unambiguous scientific value. In addition to technosignature searches, LFT3 is designed to discover previously undetected populations of low-dispersion radio transients, probing low-frequency

phenomena inaccessible from Earth. The mission opens new frontiers in radio astronomy, including low-frequency Very Long Baselines Interferometry (VLBI) with Earth-based observatories and enables the first modern detection of low-frequency radio emission from the outer planets of our Solar System, last observed by Voyager. LFT3 represents a once-in-a-generation, time-critical opportunity to listen to the radio universe in a way that has never been possible before and, if missed now, will likely never come again.

APPENDIX

A. SCIENCE TRACEABILITY MATRIX
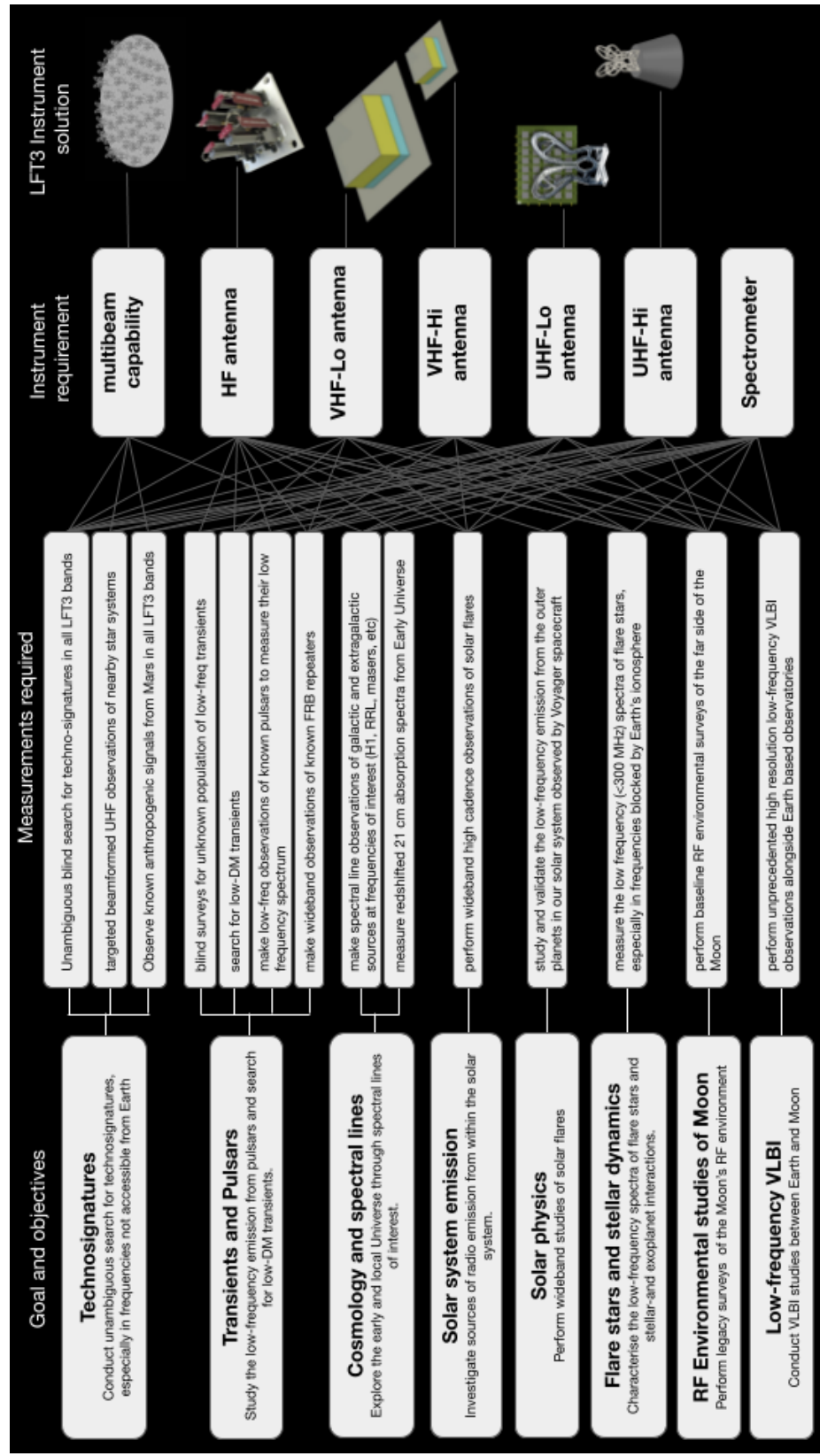
Figure 19: Science traceablity matrix for LFT3.

REFERENCES

2018, Exoplanet Science Strategy,
doi: 10.17226/25187

Adachi, S., Adkins, T., Baccigalupi, C., et al. 2024,
PhRvD, 110, 063013,
doi: 10.1103/PhysRevD.110.063013

Agazie, G., Anumarlapudi, A., Archibald, A. M., et al.
2023, The Astrophysical Journal Letters, 951, L8,
doi: 10.3847/2041-8213/acdac6

Alexander, J. K., Kaiser, M. L., Novaco, J. C., Grena,
F. R., & Weber, R. R. 1975, A&A, 40, 365

An, H., Ge, S., Liu, J., & Liu, M. 2025, PhRvL, 134,
171001, doi: 10.1103/PhysRevLett.134.171001

Anderson, L. D., Luisi, M., Liu, B., et al. 2021, ApJS,
254, 28, doi: 10.3847/1538-4365/abef65

Archibald, R. F., Gotthelf, E. V., Ferdman, R. D., et al.
2016, ApJL, 819, L16,
doi: 10.3847/2041-8205/819/1/L16

Atkinson, J. 2025, NASA Cameras on Blue Ghost
Capture First-of-its-Kind Moon Landing Footage,
Web Page. https://www.nasa.gov/general/
nasa-cameras-on-blue-ghost-capture-first-of-its-kind-\
moon-landing-footage/

Bale, S. D. 2023, in AGU Fall Meeting Abstracts, Vol.
2023, P31B–02

Bale, S. D., Bassett, N., Burns, J. O., et al. 2023a, in
URSI International Union of Radio Science General
Assembly and Scientific Symposium URSI GASS,
Sapporo, Japan

Bale, S. D., Bassett, N., Burns, J. O., et al. 2023b,
arXiv e-prints, arXiv:2301.10345,
doi: 10.48550/arXiv.2301.10345

Bandyopadhyay, S., Mcgarey, P., Goel, A., et al. 2021,
in 2021 IEEE Aerospace Conference (50100), 1–25,
doi: 10.1109/AERO50100.2021.9438165

Bassa, C. G., Di Vruno, F., Winkel, B., et al. 2024,
A&A, 689, L10,
doi: 10.1051/0004-6361/202451856

Bassett, N., Rapetti, D., Burns, J. O., Tauscher, K., &
MacDowall, R. 2020, Advances in Space Research,
66, 1265, doi: 10.1016/j.asr.2020.05.050

Bastian, T. S., Pick, M., Kerdraon, A., Maia, D., &
Vourlidas, A. 2001, ApJL, 558, L65,
doi: 10.1086/323421

Basu, A., Graber, V., Lower, M. E., et al. 2025

Batygin, K. 2018, AJ, 155, 178,
doi: 10.3847/1538-3881/aab54e

Batygin, K., & Stevenson, D. J. 2010, ApJL, 714,
L238, doi: 10.1088/2041-8205/714/2/L238

Beltz, H., Rauscher, E., Kempton, E. M. R., Malsky, I.,
& Savel, A. B. 2023, AJ, 165, 257,
doi: 10.3847/1538-3881/acd24d

Beskin, V. S., Chernov, S. V., Gwinn, C. R., &
Tchekhovskoy, A. 2015, Space Science Reviews,
191, 207, doi: 10.1007/s11214-015-0173-8

Bhat, N. D. R., Cordes, J. M., Chatterjee, S., & Lazio,
T. J. W. 2005, Radio Science, 40, RS5S14,
doi: 10.1029/2004RS003172

Bloot, S., Vedantham, H. K., Bassa, C. G., et al. 2025,
A&A, 699, A341,
doi: 10.1051/0004-6361/202555131

Bochenek, C. D., Ravi, V., Belov, K. V., et al. 2020,
NAT, 587, 59, doi: 10.1038/s41586-020-2872-x

Brain, D. A., Kao, M. M., & O'Rourke, J. G. 2024,
arXiv e-prints, arXiv:2404.15429,
doi: 10.48550/arXiv.2404.15429

Brinkerink, C. D., Arts, M. J., Bentum, M. J., et al.
2025, The Dark Ages Explorer (DEX): a
filled-aperture ultra-long wavelength radio
interferometer on the lunar far side, arXiv,
doi: 10.48550/arXiv.2504.03418

Buhler, C. R., Johansen, M., Dupuis, M., et al. 2020, in
Lunar Dust 2020, LPI Contribution No. 2243 (Lunar
and Planetary Institute). https://www.hou.usra.edu/
meetings/lunardust2020/pdf/5027.pdf

Burke-Spolaor, S., Johnston, S., Bailes, M., et al. 2012,
MNRAS, 423, 1351,
doi: 10.1111/j.1365-2966.2012.20998.x

Burns, J., Bale, S., Bradley, R., et al. 2021a, arXiv
e-prints, arXiv:2103.05085,
doi: 10.48550/arXiv.2103.05085

Burns, J., Hallinan, G., Chang, T.-C., et al. 2021b, A
Lunar Farside Low Radio Frequency Array for Dark
Ages 21-cm Cosmology.
https://arxiv.org/abs/2103.08623

Burns, J. O. 2021, Philosophical Transactions of the
Royal Society of London Series A, 379, 20190564,
doi: 10.1098/rsta.2019.0564

Caleb, M., & Keane, E. 2021, Universe, 7, 453,
doi: 10.3390/universe7110453

Callingham, J. R., Pope, B. J. S., Feinstein, A. D., et al.
2021, Astronomy & Astrophysics, 648, A13,
doi: 10.1051/0004-6361/202039144

Callingham, J. R., Pope, B. J. S., Kavanagh, R. D.,
et al. 2024, Nature Astronomy

Chadha-Day, F., Ellis, J., & Marsh, D. J. E. 2022, Science Advances, 8, eabj3618, doi: 10.1126/sciadv.abj3618

Chael, A. A., Johnson, M. D., Bouman, K. L., et al. 2018, ApJ, 857, 23, doi: 10.3847/1538-4357/aab6a8

CHIME/FRB Collaboration, Andersen, B. C., Bandura, K. M., et al. 2020, Nature, 587, 54, doi: 10.1038/s41586-020-2863-y

Cordes, J. M., & McLaughlin, M. A. 2003, ApJ, 596, 1142, doi: 10.1086/378231

Cordun, C. M., Vedantham, H. K., Brentjens, M. A., & van der Tak, F. F. S. 2025, A&A, 693, A162, doi: 10.1051/0004-6361/202452868

Cuntz, M., Saar, S. H., & Musielak, Z. E. 2000, ApJl, 533, L151, doi: 10.1086/312609

Czech, D., Isaacson, H., Pearce, L., et al. 2021, 133, 064502, doi: 10.1088/1538-3873/abf329

Dang, S.-j., Wu, Z.-w., Lu, J.-g., et al. 2025, ApJ, 988, 11, doi: 10.3847/1538-4357/ade23a

DeBoer, D. R., Parsons, A. R., Aguirre, J. E., et al. 2017, PASP, 129, 045001, doi: 10.1088/1538-3873/129/974/045001

Desch, M. D., & Barrow, C. H. 1984, Journal of Geophysical Research: Space Physics, 89, 6819, doi: https://doi.org/10.1029/JA089iA08p06819

Dickey, J. M., & Lockman, F. J. 1990, ARA&A, 28, 215, doi: 10.1146/annurev.aa.28.090190.001243

Dowell, J., & Taylor, G. B. 2018, ApJL, 858, L9, doi: 10.3847/2041-8213/aabf86

Driessen, L. N., Pritchard, J., Murphy, T., et al. 2024, Publications of the Astronomical Society of Australia, 41, e084, doi: 10.1017/pasa.2024.72

Egan, H., Jarvinen, R., Ma, Y., & Brain, D. 2019, MNRAS, 488, 2108, doi: 10.1093/mnras/stz1819

Ehman, J. 2008, The Big Ear Wow! Signal. http://www.bigear.org/wow20th.htm

Ellingson, S. W. 2005, RFI Mitigation and the SKA, ed. P. J. Hall (Dordrecht: Springer Netherlands), 261–267, doi: 10.1007/1-4020-3798-8_24

Enriquez, J. E., Siemion, A., Foster, G., et al. 2017, ApJ, 849, 104, doi: 10.3847/1538-4357/aa8d1b

EPTA Collaboration, InPTA Collaboration, Antoniadis, J., et al. 2023, A&A, 678, A50, doi: 10.1051/0004-6361/202346844

Event Horizon Telescope Collaboration, Akiyama, K., et al. 2019, ApJL, 875, L1, doi: 10.3847/2041-8213/ab0ec7

Fallows, R. A., Bisi, M. M., Forte, B., et al. 2016, The Astrophysical Journal, 828, L7, doi: 10.3847/2041-8205/828/1/L7

Fallows, R. A., Iwai, K., Jackson, B. V., et al. 2023, Advances in Space Research, 72, 5311, doi: 10.1016/j.asr.2022.08.076

Fialkov, A., Gessey-Jones, T., & Dhanda, J. 2024, Philosophical Transactions of the Royal Society A: Mathematical, Physical and Engineering Sciences, 382, doi: 10.1098/rsta.2023.0068

Firefly Aerospace. 2025, Blue Ghost Mission 1, Web Page. https://fireflyspace.com/missions/blue-ghost-mission-1/

Fritz, A., Breeding, S., & Tamasy, G. 2024, in Lunar Surface Innovation Consortium (LSIC) Fall Meeting (Las Vegas, NV: Johns Hopkins University Applied Physics Laboratory). https://ntrs.nasa.gov/api/citations/20240013978/downloads/NASA%20Lunar%20Dust%20Mitigation%20Roadmap%20Fall%202024.pdf

Gajjar, V., & Brown, G. C. 2025, Submitted

Gajjar, V., Perez, K. I., Siemion, A. P. V., et al. 2021, AJ, 162, 33, doi: 10.3847/1538-3881/abfd36

Goldreich, P., & Lynden-Bell, D. 1969, ApJ, 156, 59, doi: 10.1086/149947

Gordon, M. A., & Sorochenko, R. L., eds. 2009, Astrophysics and Space Science Library, Vol. 282, Radio Recombination Lines, doi: 10.1007/978-0-387-09604-9

Gray, R. H. 2020, AJ, 159, 228, doi: 10.3847/1538-3881/ab792b

Grießmeier, J.-M. 2015, in Astrophysics and Space Science Library, Vol. 411, Astrophysics and Space Science Library, ed. H. Lammer & M. Khodachenko, 213, doi: 10.1007/978-3-319-09749-7_11

Grießmeier, J.-M. 2017, in Planetary Radio Emissions VIII, ed. G. Fischer, G. Mann, M. Panchenko, & P. Zarka (Austrian Academy of Sciences Press, Vienna), 285–300

Grießmeier, J.-M., Tabataba-Vakili, F., Stadelmann, A., Grenfell, J. L., & Atri, D. 2015, A&A, 581, A44, doi: 10.1051/0004-6361/201425451

Grießmeier, J.-M., Zarka, P., & Spreeuw, H. 2007, A&A, 475, 359, doi: 10.1051/0004-6361:20077397

Grigg, D., Tingay, S., & Sokolowski, M. 2025, arXiv e-prints, arXiv:2506.02831, doi: 10.48550/arXiv.2506.02831

Hallinan, G., Antonova, A., Doyle, J. G., et al. 2006, The Astrophysical Journal, 653, 690, doi: 10.1086/508678

Haqq-Misra, J., Vidal, C., & Profitiliotis, G. 2025, Acta Astronautica, 229, 831, doi: 10.1016/j.actaastro.2025.01.048

Hassall, T. E., Stappers, B. W., Hessels, J. W. T., et al. 2012, Astronomy and Astrophysics, 543, A66, doi: 10.1051/0004-6361/201218970

Heidmann, J. 2002, Acta Astronautica, 50, 59, doi: 10.1016/S0094-5765(01)00139-4

HI4PI Collaboration, Ben Bekhti, N., Flöer, L., et al. 2016, A&A, 594, A116, doi: 10.1051/0004-6361/201629178

Hibbard, J. J., Burns, J. O., MacDowall, R., et al. 2025, arXiv e-prints, arXiv:2503.09842, doi: 10.48550/arXiv.2503.09842

Hippke, M., & Forgan, D. H. 2017, arXiv e-prints, arXiv:1712.06639, doi: 10.48550/arXiv.1712.06639

Hobbs, G., Manchester, R. N., Dunning, A., et al. 2020, PASA, 37, e012, doi: 10.1017/pasa.2020.2

Huang, B.-L., Tao, Z.-Z., & Zhang, T.-J. 2023, AJ, 166, 245, doi: 10.3847/1538-3881/ad06b1

Hubbard, W. B., & Smoluchowski, R. 1973, SSRv, 14, 599, doi: 10.1007/BF00166644

Hurley-Walker, N., Zhang, X., Bahramian, A., et al. 2022, Nature, 601, 526, doi: 10.1038/s41586-021-04272-x

Hurley-Walker, N., McSweeney, S. J., Bahramian, A., et al. 2024, ApJL, 976, L21, doi: 10.3847/2041-8213/ad890e

Ilin, E., & Poppenhaeger, K. 2022, MNRAS, 513, 4579, doi: 10.1093/mnras/stac1232

Ilin, E., Poppenhäger, K., Chebly, J., Ilić, N., & Alvarado-Gómez, J. D. 2024, MNRAS, 527, 3395, doi: 10.1093/mnras/stad3398

ITU. 2024, Radio Regulations, Edition of 2024. https://www.itu.int/pub/r-reg

Ivanov, M. M., Kovalev, Y. Y., Lister, M. L., et al. 2019, JCAP, 2019, 059, doi: 10.1088/1475-7516/2019/02/059

Jacob, A. M., Nandakumar, M., Roy, N., et al. 2024, A&A, 692, A164, doi: 10.1051/0004-6361/202449603

Jankowski, F., van Straten, W., Keane, E. F., et al. 2018, Monthly Notices of the Royal Astronomical Society, 473, 4436, doi: 10.1093/mnras/stx2476

Jia, S., Zhong, W., & Yu, C. 2023, ApJ, 951, 116, doi: 10.3847/1538-4357/acd4bc

Jia, Y., Zou, Y., Ping, J., et al. 2018, Planetary and Space Science, 162, 207, doi: https://doi.org/10.1016/j.pss.2018.02.011

Kaiser, M. L., Zarka, P., Desch, M. D., & Farrell, W. M. 1991, J. Geophys. Res., 96, 19043, doi: 10.1029/91JA01599

Kansabanik, D., Oberoi, D., & Mondal, S. 2022, ApJ, 932, 110, doi: 10.3847/1538-4357/ac6758

Kantharia, N. G., & Anantharamaiah, K. R. 2001, Journal of Astrophysics and Astronomy, 22, 51, doi: 10.1007/BF02933590

Kao, M. M., Mioduszewski, A. J., Villadsen, J., & Shkolnik, E. L. 2023, Nature, 619, 272, doi: 10.1038/s41586-023-06138-w

Kaplan, D. L., Tingay, S. J., Manoharan, P. K., et al. 2015, The Astrophysical Journal, 809, L12, doi: 10.1088/2041-8205/809/1/L12

Karuppusamy, R., Stappers, B. W., & van Straten, W. 2010, Astronomy and Astrophysics, 515, A36, doi: 10.1051/0004-6361/200913729

Keane, E. F. 2013, in IAU Symposium, Vol. 291, Neutron Stars and Pulsars: Challenges and Opportunities after 80 years, ed. J. van Leeuwen, 295–300, doi: 10.1017/S1743921312023927

Keller, A., Wolff, N., & van Bibber, K. 2025, ApJL, 984, L24, doi: 10.3847/2041-8213/adc9aa

Kirsten, F., Marcote, B., Nimmo, K., et al. 2022, Nature, 602, 585, doi: 10.1038/s41586-021-04354-w

Kogut, A., Fixsen, D. J., Levin, S. M., et al. 2011, ApJ, 734, 4, doi: 10.1088/0004-637X/734/1/4

Kondratiev, V. 2013, Proceedings of the International Astronomical Union, 8, 47–52, doi: 10.1017/S1743921312023125

Kopparapu, R. K., Wolf, E. T., & Meadows, V. S. 2020, in Planetary Astrobiology, ed. V. S. Meadows, G. N. Arney, B. E. Schmidt, & D. J. Des Marais, 449, doi: 10.2458/azu_uapress_9780816540068

Kumar, A., Deller, A. T., Jain, P., & Moldón, J. 2025, arXiv e-prints, arXiv:2506.14368, doi: 10.48550/arXiv.2506.14368

Lanman, A. E., Andrew, S., Lazda, M., et al. 2024, AJ, 168, 87, doi: 10.3847/1538-3881/ad5838

Lanza, A. F. 2009, A&A, 505, 339, doi: 10.1051/0004-6361/200912367

Lazio, J., Hallinan, G., Airapetian, A., et al. 2019, BAAS, 51, 135. https://arxiv.org/abs/1803.06487

Lazio, W., T. J., Farrell, W. M., Dietrick, J., et al. 2004, ApJ, 612, 511, doi: 10.1086/422449

Leung, C., Mena-Parra, J., Masui, K., et al. 2021, AJ, 161, 81, doi: 10.3847/1538-3881/abd174

Levin, L., Bailes, M., Barsdell, B. R., et al. 2013, MNRAS, 434, 1387, doi: 10.1093/mnras/stt1103

Liang, R., Deng, F., Yang, Z., et al. 2023, Research in Astronomy and Astrophysics, 23, 115006, doi: 10.1088/1674-4527/acd0ed

Lorimer, D. R., & Kramer, M. 2004, Handbook of Pulsar Astronomy, Vol. 4 (Cambridge University Press)

Louis, C. K., Loh, A., Zarka, P., et al. 2025, arXiv e-prints, arXiv:2503.18733, doi: 10.48550/arXiv.2503.18733

Louis, C. K., Louarn, P., Collet, B., et al. 2023, Journal of Geophysical Research (Space Physics), 128, e2023JA031985, doi: 10.1029/2023JA031985

Lovelace, R. V. E., Romanova, M. M., & Barnard, A. W. 2008, MNRAS, 389, 1233, doi: 10.1111/j.1365-2966.2008.13617.x

Luan, X.-H., Tao, Z.-Z., Zhao, H.-C., et al. 2023, AJ, 165, 132, doi: 10.3847/1538-3881/acb706

Lynch, C., Murphy, T., Ravi, V., et al. 2016, Monthly Notices of the Royal Astronomical Society, 457, 1224, doi: 10.1093/mnras/stw050

Lynch, C. R., Murphy, T., Lenc, E., & Kaplan, D. L. 2018, MNRAS, 478, 1763, doi: 10.1093/mnras/sty1138

Lyne, A. G., Burgay, M., Kramer, M., et al. 2004, Science, 303, 1153, doi: 10.1126/science.1094645

Maccone, C. 2019, Acta Astronautica, 154, 233, doi: https://doi.org/10.1016/j.actaastro.2018.02.012

Manchester, R. N., Hobbs, G. B., Teoh, A., & Hobbs, M. 2005, AJ, 129, 1993, doi: 10.1086/428488

McKay, D. S., Heiken, G., Basu, A., et al. 1991, The Lunar Regolith, ed. G. H. Heiken, D. T. Vaniman, & B. M. French (Cambridge: Cambridge University Press), 285–356. https://www.lpi.usra.edu/publications/books/lunar_sourcebook/

Meiksin, A. 2002, in IAU Symposium, Vol. 199, The Universe at Low Radio Frequencies, ed. A. Pramesh Rao, G. Swarup, & Gopal-Krishna, 71

Men, Y., McSweeney, S., Hurley-Walker, N., Barr, E., & Stappers, B. 2025, Science Advances, 11, eadp6351, doi: 10.1126/sciadv.adp6351

Méndez, A., Ortiz Ceballos, K., & Zuluaga, J. I. 2024, arXiv e-prints, arXiv:2408.08513, doi: 10.48550/arXiv.2408.08513

Michaud, E. J., Siemion, A. P. V., Drew, J., & Worden, S. P. 2020, Lunar Opportunities for SETI. https://arxiv.org/abs/2009.12689

Ng, C. 2023, A brief review on Fast Radio Bursts, arXiv, doi: 10.48550/arXiv.2311.01899

Nimmo, K., Hessels, J. W. T., Snelders, M. P., et al. 2023, Monthly Notices of the Royal Astronomical Society, 520, 2281, doi: 10.1093/mnras/stad269

Offringa, A. R., Wayth, R. B., Hurley-Walker, N., et al. 2015, PASA, 32, e008, doi: 10.1017/pasa.2015.7

Paul, S., Santos, M. G., Chen, Z., & Wolz, L. 2023, arXiv e-prints, arXiv:2301.11943, doi: 10.48550/arXiv.2301.11943

Payne-Scott, R., Yabsley, D. E., & Bolton, J. G. 1947, Nature, 160, 256, doi: 10.1038/160256b0

Perez, K. I., Farah, W., Sheikh, S. Z., et al. 2022, Research Notes of the American Astronomical Society, 6, 197, doi: 10.3847/2515-5172/ac9408

Perna, R., Menou, K., & Rauscher, E. 2010, ApJ, 719, 1421, doi: 10.1088/0004-637X/719/2/1421

Pietka, M., Fender, R. P., & Keane, E. F. 2015, MNRAS, 446, 3687, doi: 10.1093/mnras/stu2335

Pineda, J. S., & Villadsen, J. 2023, Nature Astronomy, 7, 569, doi: 10.1038/s41550-023-01914-0

Pingel, N. M., Dempsey, J., McClure-Griffiths, N. M., Dickey, J. M., et al. 2022, PASA, 39, e005, doi: 10.1017/pasa.2021.59

Piro, L., Bruni, G., Troja, E., et al. 2021, A&A, 656, L15, doi: 10.1051/0004-6361/202141903

Pleunis, Z., Michilli, D., Bassa, C. G., et al. 2021, ApJL, 911, L3, doi: 10.3847/2041-8213/abec72

Pospelov, M., Pradler, J., Ruderman, J. T., & Urbano, A. 2018, PhRvL, 121, 031103, doi: 10.1103/PhysRevLett.121.031103

Prabu, S., DeBoer, D., & Ashe, C. 2025a, LFT3 Science Operations, Memo 2, LFT3 Project

Prabu, S., DeBoer, D., & Siemion, A. 2025b, LFT3 Star Catalog, Memo 3, LFT3 Project

Price, D. C. 2016, PyGDSM: Python interface to Global Diffuse Sky Models, Astrophysics Source Code Library, record ascl:1603.013

Price, D. C., Enriquez, J. E., Brzycki, B., et al. 2020, AJ, 159, 86, doi: 10.3847/1538-3881/ab65f1

Reardon, D. J., Zic, A., Shannon, R. M., et al. 2023, ApJL, 951, L6, doi: 10.3847/2041-8213/acdd02

Ren, X., Yan, W., Zeng, X., et al. 2025, Nature Communications, 16, Article number: 59443, doi: 10.1038/s41467-025-59443-5

Rhee, J., Meyer, M., Popping, A., et al. 2023, MNRAS, 518, 4646, doi: 10.1093/mnras/stac3065

Rosa, I., Roedel, H., Allende, M. I., Lepech, M. D., & Loftus, D. J. 2020, Journal of Renewable Materials, 8, 845, doi: 10.32604/jrm.2020.09844

Route, M. 2019, ApJ, 872, 79, doi: 10.3847/1538-4357/aafc25

Saide, R. C., Garrett, M. A., & Heeralall-Issur, N. 2023, MNRAS, 522, 2393, doi: 10.1093/mnras/stad378

Salas, P., Oonk, J. B. R., Emig, K. L., et al. 2019, A&A, 626, A70, doi: 10.1051/0004-6361/201834532

Salas, P., Oonk, J. B. R., van Weeren, R. J., et al. 2018, MNRAS, 475, 2496, doi: 10.1093/mnras/stx3340

Salter, D. M., Hogerheijde, M. R., & Blake, G. A. 2008, A&A, 492, L21, doi: 10.1051/0004-6361:200810807

Selina, R., & De Pree, C. 2023, Detrimental Emission Levels for Orbital RFI, Technical Memorandum RFI Memo 153, ngVLA Memo 119, National Radio Astronomy Observatory (NRAO)

Shahar, A., Driscoll, P., Weinberger, A., & Cody, G. 2019, Science, 364, 434, doi: 10.1126/science.aaw4326

Sheikh, S. Z., Huston, M. J., Fan, P., et al. 2025, AJ, 169, 118, doi: 10.3847/1538-3881/ada3c7

Sheikh, S. Z., Smith, S., Price, D. C., et al. 2021, Nature Astronomy, 5, 1153, doi: 10.1038/s41550-021-01508-8

Sheldahl, E. E., Taylor, G. B., Tremblay, S. E., et al. 2025, ApJ, 987, 26, doi: 10.3847/1538-4357/adcc28

Shinnaga, H., Oyadomari, M., Imai, H., et al. 2025, PASJ, doi: 10.1093/pasj/psaf013

Stappers, B. W., Hessels, J. W. T., Alexov, A., et al. 2011, A&A, 530, A80, doi: 10.1051/0004-6361/201116681

Susarla, S. C., Chalumeau, A., Tiburzi, C., et al. 2024, A&A, 692, A18, doi: 10.1051/0004-6361/202450680

Thorngren, D. P., & Fortney, J. J. 2018, AJ, 155, 214, doi: 10.3847/1538-3881/aaba13

Tremblay, C. D., Hurley-Walker, N., Cunningham, M., et al. 2017, MNRAS, 471, 4144, doi: 10.1093/mnras/stx1838

Tremblay, C. D., Jordan, C. H., Cunningham, M., Jones, P. A., & Hurley-Walker, N. 2018, PASA, 35, e018, doi: 10.1017/pasa.2018.13

Tremblay, C. D., Price, D. C., & Tingay, S. J. 2022, PASA, 39, e008, doi: 10.1017/pasa.2022.5

Tremblay, C. D., Gray, M. D., Hurley-Walker, N., et al. 2020, ApJ, 905, 65, doi: 10.3847/1538-4357/abc33a

Tremblay, C. D., Varghese, S. S., Hickish, J., et al. 2024, AJ, 167, 35, doi: 10.3847/1538-3881/ad0fe0

Trigilio, C., Biswas, A., Leto, P., et al. 2023, arXiv e-prints, arXiv:2305.00809, doi: 10.48550/arXiv.2305.00809

Turner, J. D., Christie, D., Arras, P., Johnson, R. E., & Schmidt, C. 2016, MNRAS, 458, 3880, doi: 10.1093/mnras/stw556

Turner, J. D., Grießmeier, J.-M., Zarka, P., & Vasylieva, I. 2019, A&A, 624, A40, doi: 10.1051/0004-6361/201832848

Turner, J. D., Grießmeier, J.-M., Zarka, P., Zhang, X., & Mauduit, E. 2024, A&A, 688, A66, doi: 10.1051/0004-6361/202450095

Turner, J. D., Zarka, P., Grießmeier, J.-M., et al. 2021, A&A, 645, A59, doi: 10.1051/0004-6361/201937201

—. 2023, Planetary, Solar and Heliospheric Radio Emissions IX, doi: https://doi.org/10.25546/104048

Tyrrell, O. K., Thompson, R. J., Danehy, P. M., et al. 2022, in AIAA SciTech Forum (San Diego, CA, USA: American Institute of Aeronautics and Astronautics). https://ntrs.nasa.gov/citations/20210024671

Valio, A., Kaufmann, P., Giménez de Castro, C. G., et al. 2013, SoPh, 283, 651, doi: 10.1007/s11207-013-0237-4

van Haarlem, M. P., Wise, M. W., Gunst, A. W., et al. 2013, A&A, 556, A2, doi: 10.1051/0004-6361/201220873

Vasavada, A. R., Bandfield, J. L., Greenhagen, B. T., et al. 2012, Journal of Geophysical Research (Planets), 117, E00H18, doi: 10.1029/2011JE003987

Villadsen, J., & Hallinan, G. 2019, The Astrophysical Journal, 871, 214, doi: 10.3847/1538-4357/aaf88e

Voyager Technologies. 2025, Voyager's Clear Dust-Repellent Coating Lands on the Moon, https://voyagertechnologies.com/press-releases/voyagers-clear-dust-repellent-coating-lands-on-the-moon/

Vydula, A. K., Bowman, J. D., Lewis, D., et al. 2024, AJ, 167, 2, doi: 10.3847/1538-3881/ad08ba

Wang, Y.-C., Cipriani, F., Johansson, F. L., Sperl, M., & Adachi, M. 2024, Advances in Space Research, 74, 6194, doi: https://doi.org/10.1016/j.asr.2024.07.082

Wild, J. P., Smerd, S. F., & Weiss, A. A. 1963, ARA&A, 1, 291, doi: 10.1146/annurev.aa.01.090163.001451

Wimmer-Schweingruber, R. F., Yu, J., Böttcher, S. I., et al. 2020, arXiv preprint arXiv:2001.11028. https://arxiv.org/abs/2001.11028

Worden, P. 2016, in 67th International Astronautical Congress 2016, 34378

Yan, J., Wu, J., Gurvits, L. I., et al. 2023, Experimental Astronomy, 56, 333, doi: 10.1007/s10686-022-09887-0

Zanon, P., Dunn, M., & Brooks, G. 2023, Acta Astronautica, 213, 627, doi: https://doi.org/10.1016/j.actaastro.2023.09.031

Zarka, P. 1998, Journal of Geophysical Research: Planets, 103, 20159, doi: 10.1029/98JE01323

Zarka, P. 2007, P&SS, 55, 598, doi: 10.1016/j.pss.2006.05.045

—. 2018, Star-Planet Interactions in the Radio Domain: Prospect for Their Detection, ed. H. J. Deeg & J. A. Belmonte, 22, doi: 10.1007/978-3-319-55333-7_2210.1007/978-3-319-30648-3_22-1

Zarka, P., Farrell, W., Fischer, G., & Konovalenko, A. 2008, SSRv, 137, 257, doi: 10.1007/s11214-008-9366-8

Zarka, P., Farrell, W. M., Kaiser, M. L., Blanc, E., & Kurth, W. S. 2004, Planet. Space Sci., 52, 1435, doi: 10.1016/j.pss.2004.09.011

Zarka, P., Lazio, J., & Hallinan, G. 2015, Advancing Astrophysics with the Square Kilometre Array (AASKA14), 120

Zarka, P., & Pedersen, B. M. 1986, Nature, 323, 605, doi: 10.1038/323605a0

Zawdie, K. A., Drob, D. P., Siskind, D. E., & Coker, C. 2017, Radio Science, 52, 767, doi: https://doi.org/10.1002/2017RS006256

Zhang, M., Belcher, J., & McNutt, R. 1992, Advances in Space Research, 12, 37, doi: https://doi.org/10.1016/0273-1177(92)90421-S

Zhang, S. B., Geng, J. J., Wang, J. S., et al. 2024, ApJ, 972, 59, doi: 10.3847/1538-4357/ad6602

Zhang, X. 2025, in Radio Frequency Interference Conference, 46

Zhang, X., Zarka, P., Girard, J. N., et al. 2025a, arXiv e-prints, arXiv:2506.07912, doi: 10.48550/arXiv.2506.07912

Zhang, X., Zarka, P., Viou, C., et al. 2025b, arXiv e-prints, arXiv:2504.10032, doi: 10.48550/arXiv.2504.10032

Zhelezniakov, V. V., & Zlotnik, E. I. 1975, 43, 431, doi: 10.1007/BF00152366